

The Endocytic Protein FCHO-1 is Essential in Preserving the Structural and Functional Integrity of Neurons

Monet Andrea Jimenez

A dissertation

submitted in partial fulfillment of the

requirements for the degree of

Doctor of Philosophy

University of Washington

2023

Reading Committee:

Jihong Bai, Chair

Suman Jayadev

Jessica Young

Program Authorized to Offer Degree:

Pathology

©Copyright 2023

Monet Andrea Jimenez

University of Washington

Abstract

The Endocytic Protein FCHO-1 is Essential in Preserving the Structural and Functional Integrity of Neurons

Monet Andrea Jimenez

Chair of the Supervisory Committee:

Jihong Bai

Biochemistry

Neurons are vital for animal physiology and behavior, demanding lifelong structural and functional integrity. This integrity is upheld by intricate endocytic pathways that sustain a multitude of critical neuronal features, such as cell polarity, circuit formation and maintenance, and rapid neurotransmission between neurons and their target cells. However, the precise convergence of these diverse pathways, comprising both unique and shared endocytic proteins, to collectively support the overall health of neurons remains elusive. In this thesis, I investigated the role of FCHO-1, a key endocytic protein, in *C. elegans* neurons. My studies revealed a remarkable and unexpected facet of FCHO-1, involving the preservation of neuronal structure and function. I showed that *fcho-1 null* mutant worms exhibited only moderate reductions in synaptic transmission strength and slightly diminished synaptic vesicle abundance — a surprising revelation. However, using electron microscope analysis, I found a distinct phenomenon: numerous abnormal “breaks” on the plasma membranes between neurons, suggestive of

compromised neuronal boundaries. To delve deeper into this finding, I introduced a novel PAGEN assay, a fluorescence imaging method enabling quantification of cytoplasmic content exchange among live neurons. Using this method, I demonstrated that compromised neuronal membrane contacts in *fcho-1* mutant worms allow for an elevated occurrence of abnormal cytoplasmic content exchange among neurons. Furthermore, I found that accumulation of adhesion molecule SYG-1 is increased in *fcho-1* mutant neurons, comparing to wild type neurons. Collectively, these findings reveal FCHO-1's critical and previously recognized role in maintaining neuron boundaries. This likely occurs through influencing the abundance of adhesion molecules on neuronal membranes, thereby potentially impacting the rigidity and stability of neuron-neuron contacts. In summary, my research uncovers an unexpected facet of the FCHO-1-dependent endocytic pathway — its pivotal role in preserving neuronal structural integrity.

TABLE OF CONTENTS

<u>Chapter 1: The Role of Endocytosis in Fortifying Neuronal Integrity</u>	8
Overview of Endocytosis.....	9
Endocytosis Regulates Neuronal Polarity.....	10
Quality Control of Membrane Proteins through Endocytosis in Nuerons.....	11
<u>Chapter 2: Synaptic Vesicle Endocytosis</u>	13
Major Endocytic Pathways for Synaptic Vesicle Recycling.....	14
Same Protein, Different Pathway?.....	16
Synaptic Vesicle Recycling in <i>C.elegans</i>	17
<u>Chapter 3: Clathrin-Mediated Endocytosis: The Road Most Travelled</u>	19
The Molecular Center of CME: The Adaptor Protein AP-2.....	20
To Initiate or to Not: The Endocytic Protein FCHO-1 contributes to CME.....	22
Disrupted Endocytosis: Implications for Neurodegenerative Disorders.....	23
<u>Chapter 4: Key Findings in Thesis Research</u>	26
<u>Chapter 5: FCHO-1 Functions Through an AP-2 Mediated Pathway That is Necessary to Maintain the Structural Integrity of Neuronal Membranes</u>	27
Introduction.....	28
Results.....	31
Figures.....	41
Discussion.....	55
Supplementary Figures.....	60
Materials and Methods.....	64
<u>Chapter 7: Conclusions and Future Directions</u>	70
<u>Chapter 8: Bibliography</u>	75

DEDICATION

This thesis is dedicated to my mom, my grandma, my nieces, and nephew, my cat Pickles, my family, and the friends both near and far who kept me balanced.

I like to believe that the culmination of my academic journey began 22 years ago when my grandmother made the decision to return to school to pursue her teaching degree. As my caretaker, she had no option but to bring me along to her classes at our local community college. We must have appeared as an unusual pair to onlookers - an elderly college student and her 8-year-old granddaughter, united in the quest to decipher Algebra. My grandmother instilled in me, from a young age, the significance of education and, more importantly, the belief that it is only impossible if we allow it to be. She proudly displayed my accolades around her home, celebrating them as if they were her own. Her unwavering support and enthusiasm for my years as a scholar were constants that I carried with me throughout my journey, something I relied upon to keep pushing forward. Completing this thesis marks the conclusion of a journey filled with dreams that once seemed unattainable - we did it granny goose.

Mom, I extend my heartfelt gratitude for standing by me every step of the way, from driving me to San Francisco to navigating mountainous roads five years later as we embarked on my journey here in Seattle. It is through your guidance that I learned the value of hard work and the motto of "always find a way."

To everyone who has played a role, be it significant or subtle, in shaping me along this journey: Thank you. This Ph.D. is as much yours as it is mine. I hold deep affection for each and every one of you.

ACKNOWLEDGEMENTS

I would like to express my sincere gratitude to my PhD advisor, Dr. Jihong Bai. Your guidance, patience, and unwavering commitment to the scientific pursuit have been instrumental in shaping my journey. Thank you for believing in me and for going above and beyond in your role as a mentor. It's because of your support and the nurturing environment you fostered here in Seattle that I rediscovered my passion for science.

My heartfelt thanks extend to the entire Bai Lab. You have become an extended family to me, and I always felt a sense of belonging and comfort in your presence. Special appreciation goes to Lin Zhang, Yan Lui, and Cera Hassain, who have made a significant impact on my life, just as I hope I have on yours.

I am deeply grateful to the members of my committee, Dr. Susan Biggins, Dr. Jessica Young, Dr. Elizabeth Nance, and Dr. Suman Jayadev. Your guidance and insightful discussions have played a crucial role in my academic journey. To my fellow graduate students in the Molecular Medicine and Mechanisms of Disease (M3D) program, you have been my pillar of support and companions in navigating this challenging path. I also want to extend my thanks to the selection committee of M3D for providing me with the opportunity to advance in the scientific realm and evolve into the scientist I am proud to be today.

Lastly, my appreciation goes to all the funding sources that have supported my scientific pursuits throughout my time in graduate school. This includes the NIH/NINDS NRSA Predoctoral Fellowship (5F31NS118844) from 2020 to 2023, the NIH/NIGMS NIH National Institute of General Medicine Sciences Diversity Supplement (R01GM127857) from 2019 to 2020, and the NIH-T32 Molecular Medicine Training Grant (T32GM09542) from 2017 to 2019. Your support has been invaluable in allowing me to grow as a scientist and contribute to the field.

CHAPTER 1:

The Role of Endocytosis in Fortifying Neuronal Integrity

Neurons possess three extraordinary attributes that distinguish them from all other cell types: structural and functional polarity among individual neuronal cells, their ability to send and receive signals at astonishingly rapid rates, and because of their post-mitotic nature, a commitment to robust performance from their inception to demise. These defining characteristics hinge upon a complex web of specialized endocytic trafficking pathways that use a varying combination of shared and specialized proteins. Over the years of extensive exploration and research, a wide range of kinetically and functionally distinct endocytic pathways have been revealed and thoroughly characterized at the ultrastructural level. However, there remains a significant gap in our understanding of the neuronal specific dynamics and molecular organization of endocytic pathways, since much of our current knowledge stems from studies conducted on non-neuronal cells [1]. In this following chapter, I will discuss the importance of some of these neuronal features and how they are driven and supported by endocytic programs.

Overview of Endocytosis

The cellular boundary between cells and their extracellular environment is established by their plasma membrane (PM). The PM is comprised of a lipid bilayer that is embedded with various proteins, which holistically functions as a protective barrier. At the PM, cells can selectively facilitate the entry and/or engulfment of various extracellular molecules, such as nutrients or signaling molecules [2, 3], or the removal of PM proteins, through a process known as endocytosis. In several instances, varying spans of the PM are simultaneously engulfed. Endocytosis is an evolutionarily conserved cellular program that is vital in all cells. During endocytosis cells organize

specialized endocytic proteins on the PM to orchestrate the engulfment, or protrusion, of the PM. These protrusions enclose the molecules destined for internalization and are subsequently pinched off the PM, forming intracellular membrane-bound vesicles. These vesicles then transport the internalized cargo to various destinations within the cell. During endocytic programs such as phagocytosis or pinocytosis, large sections of the PM are engulfed following bulk retrieval of extracellular particles or large liquid volumes, respectively. These endocytic programs are energy-intensive and the proteins along the PM are internalized in a nonspecific manner[4]. However, cells have developed a specialized program termed receptor-mediated endocytosis (RME) for the targeted uptake of PM proteins. RME employs specific membrane proteins that recruit a concentration of endocytic proteins, streamlining the internalization of cargo in an energy-efficient manner. These internalized molecules are often targeted for degradation or recycled back to the plasma membrane. Through RME, cells can regulate the precise addition and removal of proteins from the PM, fine tuning how they interact with their extracellular environment. While both bulk and receptor-mediated endocytic programs are relevant in neurons, I will focus on receptor-mediated endocytic pathways in the subsequent chapters. The specificity of these pathways grants insight to how these distinctive neuronal features may be differentially regulated and maintained.

Endocytosis Regulates Neuronal Polarity

Neurons possess a distinct polarized morphology, comprising specialized compartments with distinct structures and functions. On one end, complex dendritic arbors retrieve incoming signals, and are spatially segregated from axonal projections

and synaptic terminals, which transmit outgoing information. Endocytic programs play a pivotal role in establishing and maintaining neuronal polarity during development and throughout adulthood[5]. During development, polarized proteins are selectively endocytosed from PMs, sorted, and delivered to their intended compartments. When the endocytic molecular machinery is disrupted, neuronal polarity is compromised due to impaired retrieval of polarized proteins and mis-sorting of plasma membrane contents, undermining domain fidelity [6-8]. Additionally, the axon initial segment (AIS), a critical junction between these functional neuronal regions, upholds a similar principle[9, 10]. Recent findings in *C. elegans* reveal that polarized receptors undergo endocytosis and subsequent degradation within the AIS [11]. Disruption of the AIS's endocytic machinery leads to mis-localized polarized proteins, disrupting cellular polarity. This underscores endocytosis as a key mechanism ensuring neuronal compartmentalization. Interestingly, endocytosis of proteins that support the AIS compartment must paradoxically be inhibited to facilitate its assembly and function [12-14]. The dual nature of endocytosis, the promotion and intentional inhibition of a subset of PM proteins is essential for upholding neuronal polarity. However, there is still much to discover regarding the regulation of these opposing acts of endocytosis.

Quality Control of Membrane Proteins through Endocytosis in Neurons

Establishing polarity within cells extends to the broader perspective of the entire neuronal cell. Neurons must also intricately manage the composition of their outer boundaries to foster efficient collaboration with neighboring cells within their neuronal circuits. To accomplish this, neurons predominantly depend on receptor-mediated

endocytic programs. During neuronal development, a precisely orchestrated interplay between guidance receptors and adhesion molecules among PM boundaries [15, 16] establishes and strengthens early neuronal circuits. As these circuits form, migrating neurons precisely coordinated processes of adhesion and deadhesion to neighboring cells, inherently involving endocytosis. For example, in elongating neural progenitor cells and neurons, synchronized endocytosis of surface guidance receptors not only guides direction but also promotes transient interactions with other cells [17-19]. In mature neurons, the endocytosis of cell adhesion molecules (CAMs) from PMs remains vital to also support synaptic plasticity [20] and to influence synapse formation, stability, and strength[21]. Additionally, endocytic recycling of CAMs and other receptor proteins from the plasma membrane is a critical regulatory mechanism to initiate, or repress, multiple intracellular signaling pathways. For instance, the insertion and internalization of neurotransmitter receptors, as well as CAMs, modulate the neurons' ability to bind to extracellular ligands, which ultimately dictates which neurons communicate in addition to the flow of communication between them [22-25]. Thus, selective endocytosis of PM membrane proteins underpins various aspects important for neuronal development which continue into adulthood to sustain neuronal signaling and the plasticity of circuit connectivity.

CHAPTER 2:

Synaptic Vesicle Endocytosis

Neurons communicate within their networks using neurotransmitters, encapsulated in specialized synaptic vesicles (SVs) that reside in their synaptic terminals. Upon stimulation, these SVs fuse with the synaptic terminal membranes, releasing neurotransmitters into the extracellular space for interaction with post-synaptic targets. After SV fusion, synaptic vesicle proteins are swiftly reclaimed from the plasma membrane through a process known as synaptic vesicle recycling [26, 27]. The efficient and timely recycling of SVs is critical for replenishing functional SVs, enabling neurons to rapidly respond to subsequent signals. It is noteworthy that while SV recycling is unique to neurons, the endocytic pathways and molecular machinery involved are largely conserved across other cell types. This notion is particularly intriguing given the imperative for distinctly rapid endocytic processing within neurons. Multiple models have been proposed for SV recycling in neurons. In this chapter, I will touch on some of the significant parallels and distinctions among these diverse endocytic pathways.

Major endocytic pathways for synaptic vesicle recycling

Currently, four major pathways for SV recycling have been described, clathrin-mediated endocytosis (CME) and clathrin-independent pathways (CIE), such as kiss-and-run (K&R), ultrafast endocytosis, and activity-dependent-bulk endocytosis (ADBE). To date, how these pathways differentially contribute to presynaptic transmission is heavily debated [28, 29]. A central difference between these pathways is their kinetics and the use of the protein clathrin, which is a triskelion-shaped scaffold protein [30-32]. There are two notable descriptive features of CME: 1) A unique coat of clathrin forms at the PM, referenced as “clathrin-coated pits,” which mark the targeted region for internalization and 2) concluding CME results in budding of intracellular clathrin-coated

vesicles. Several studies focusing on mammalian synapses have suggested that SVs are reformed from the PM via CME [33-36]. Consistent with this model, others have demonstrated that SV proteins are the major cargo retrieved from clathrin-coated vesicles at nerve terminals [37, 38] in addition to the association between SV proteins and CME proteins [39-45]. However, others debate that SV retrieval via CME is achieved by secondary budding of SVs from large endosomes which are first retrieved via bulk engulfment of the PM (ABDE, or bulk endocytosis) [46-48]. While CME activity remains enigmatic at synaptic terminals, several reports in mutant murine models lacking CME associated proteins [49-51] lead to altered synaptic activity, indicating an important link between robust CME activity and synaptic function.

Amidst debates of CME activity at synaptic terminals, SV CIE pathways were discovered, which generally, but not always, occur more rapidly than CME. CME is considered to be a relatively slow pathway, (~10-30s), which brought attention to these more rapid pathways thought to be more suited to accommodate the demanding speeds necessary to support synaptic transmission. K&R endocytosis was initially discovered upon observation of uncoated vesicles at synaptic terminals [52], and in subsequent studies it was suggested that this mode of endocytosis does not require clathrin-associated proteins [53]. It was later proposed that SV reformation occurs through fast closure of a transient fusion pore [54, 55], and takes <1–2 s to completion. Bulk endocytosis or ABDE can engulf several SV membranes within a short period of time, often resulting in the generation of very large vesicles from the PM, and often follow very intense stimulation [56-59]. It is important to note, that these endosomes are a heterogenous pool of proteins and thus not functional synaptic vesicles. Alas, ultrafast

endocytosis, which is the least understood, can function at millisecond timescales and also does not require clathrin [60, 61].

Same Protein, Different pathway?

These pathways were discovered through studies conducted on diverse model organisms, cell types, and under different temperature conditions. It's believed that these pathways exist universally but are contingent upon specific conditions. In neurons, understanding the precise interactions and regulation of varying endocytic pathways remains complex. Contributing hinderances include limitations in technology and methodology, the intricate nature of nervous systems, the presence of shared proteins across simultaneously occurring yet divergent pathways, as well as the redundancy of various endocytic proteins. For example, though poorly understood, ultrafast endocytosis (that is clathrin-independent) involves synaptojanin-1 and Endophilin-A, (*unc-26* and *unc-57* in *C.elegans*, respectively), which are two key players also required for CME [49, 62]. These proteins work synergistically to induce the tubulation of invaginated membranes [63], and subsequently cleaved from the PM by the GTPase protein, dynamin [61]. It is believed these mechanistic features are consistent in ultrafast endocytosis. Moreover, in *C. elegans* the membrane bending feature of Endophilin/UNC-57 is required for proper synaptic transmission, dually necessary at PMs and endosomes [64], suggesting Endophilin/UNC-57 is partaking in differential pathways that complementarily support synaptic transmission. Taken together, the concept of shared endocytic proteins sparks several questions in the field such as: How are these shared proteins differentially regulated and does their

functionality change between pathways? To what extent can these proteins be compensated for? And which specific instances employ which endocytic pathways?

Synaptic Vesicle Recycling in *C.elegans*

The capability to perform whole-cell patch clamping (electrophysiology experiments), on both motor neurons and muscles (NMJs) in *C. elegans* [65], catalyzed significant breakthroughs in the study of synaptic vesicle endocytosis. It made it possible to seamlessly integrate functional studies and ultrastructural analyses across various genetic contexts. In *C.elegans*, early studies had also implicated the requirement CME-associated proteins in synaptic vesicle recycling [53, 66, 67], emphasizing the critical role of CME in this process. However, as technology continued to advance, the essentiality of CME at neuromuscular junctions was brought into question with the emergence of evidence for clathrin-independent mechanisms. The combination of optogenetics and high-pressure freezing experiments on whole *C. elegans* animals revealed the accumulation of large endosome-sized vesicles in hyper-stimulated cholinergic synapses [68]. These endosome-like structures were believed to result from activity-dependent bulk endocytosis at the PM, rather than CME. Additionally, the hallmark clathrin-associated "pits" were not observed on the synaptic terminal PMs following stimulation in mutants lacking CME-associated proteins. Collectively these findings made way for the discovery of a novel endocytic route that was not reliant on clathrin. Building on this hypothesis, refinements in electron microscopy techniques later unveiled the generation of smaller uncoated endocytic vesicles shortly after stimulation. Due to its swift kinetics, this rapid endocytic route was ultimately termed ultrafast endocytosis and proposed as the predominant endocytic pathway in *C. elegans* NMJs

[61]. Subsequent studies demonstrated that this endocytic route was rampant in hyper-stimulated neurons, coalescing a rapid endocytic program suitable for rapid synaptic transmission. The revelation of ultrafast endocytosis sparked investigations in other model systems, leading to its eventual identification within a subset of mammalian neurons in addition to hyper-stimulating conditions [69, 70].

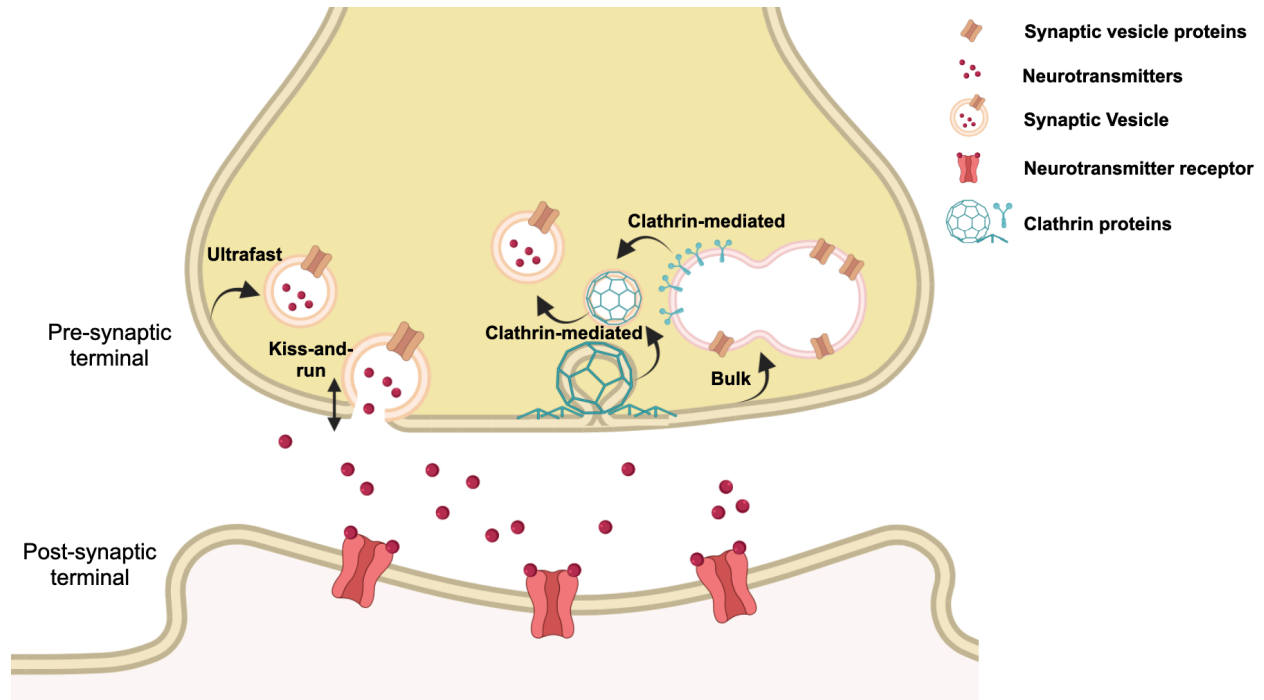


Figure 1: Several modes of synaptic vesicle (SV) endocytosis occur in neurons

There are currently four classical modes of SV endocytosis at nerve terminals known as SV recycling. Once action potentials induce SV fusion at the nerve terminal, dependent on varying factors and neuronal cell-types, SVs are commonly reconstituted through the four classical pathways: ultrafast endocytosis, kiss-and-run (K&R) clathrin-mediated endocytosis (CME), or bulk-endocytosis. The different routes are kinetically distinct and use a combination of unique and shared proteins. While some evidence supports that these pathways function simultaneously, the use of these pathways is thought to be dependent on various factors, including temperature, neuronal activity, and neuronal cell-type. Adapted from [163].

CHAPTER 3:

Clathrin-Mediated Endocytosis: The Road Most Travelled

Clathrin-mediated endocytosis (CME) is the most heavily studied and mechanistically understood endocytic pathway. To date, it is still regarded as the major pathway for targeted internalization of various proteins in all cells and across species. Given its broadly encompassing impact on multiple aspects of cellular homeostasis, the mechanisms by which cells regulate CME to support a range of functions within a single cell remain elusive. The extent of this knowledge gap is even more pronounced when it comes to CME within neurons, as studies delineating the molecular underpinnings of CME were predominantly conducted in non-neuronal cells. This void in our understanding is compounded by the intricate nature of the nervous system and the challenges associated with delineating and contextualizing the interplay between CME and the numerous concurrent endocytic pathways. In this chapter, I will introduce key molecular players that are central to CME, and the association between CME human health and disease.

The Molecular Center of CME: The Adaptor Protein AP-2

CME is orchestrated by over 50 cytosolic proteins that assemble from the cytosol to the endocytic site in a highly ordered manner [71-74]. Aforementioned, CME is notable for its generation of intracellular clathrin-coated vesicles. In one model, clathrin arrives to the PM in the early stages of CME induction, forming clathrin “pits” at endocytic sites. Interestingly, clathrin cannot bind to lipids or PM proteins directly [75], thus requiring and relying on specialized endocytic proteins called clathrin-adaptor proteins (APs), which link forming clathrin coats to the PM. APs can simultaneously bind PM proteins that are targeted for endocytosis, with specificity. In humans, 5 adaptor proteins have been identified (AP1-AP5) [76-79], while only 3 have been identified in *C.elegans* (AP-1,

AP2, & AP-3) [80-83]. It is believed that the variance of AP proteins is a contributing means to distinguish CME targets [84, 85]. However, the adaptor protein, AP-2, is the most common CME affiliate and recognized as a key component of CME. AP-2 is a heterotetrameric protein complex consisting of α , β 2, μ 2, and σ 2 subunits. Reports have suggested that the binding of AP-2 to the PM prompts clathrin assembly and the recruitment of additional endocytic proteins, thus being central to CME initiation [86, 87]. Interestingly, AP-2 undergoes two distinct conformational changes, transitioning between an active and an inactivated state. Comprehensive structural analyses of AP-2 have revealed that it is allosterically activated by interactions with FCHO-1 (Fer/Cip4 homology domain-only protein-1) in promotion of CME progression [88-90]. Conversely, AP-2 is presumed to shift into its inactivated state when it binds to the endocytic protein NECAP (adaplin-ear-binding coat-associated protein) [88, 90, 91]. In its inactivated configuration, AP-2's binding sites to PM proteins and other endocytic components, such as clathrin, become inaccessible, thereby hindering endocytic progression. Depletion of AP-2 in its entirety is fatal, thus our depiction of AP-2's function and its indispensability in CME have been restricted to experiments involving viable knockdowns of, or mutations in, the individual subunits of AP-2. In mice and flies, the mere loss of individual subunits results in embryonic lethality, demonstrating the broad essentiality of CME and the notable contributions of AP-2 in this process [92, 93]. Contrastingly, in *C.elegans*, null mutations and strong loss of function mutations of individual AP-2 subunits are viable. The viability of these AP-2 mutations has facilitated an intricate examination of CME, leading to valuable insights into the variations in CME among different cell types and species.

To Initiate or to Not: The Endocytic Protein FCHO-1 Contributes to CME

Another star CME affiliate is the endocytic protein FCHO-1 belonging to muniscin family of proteins. In vertebrates, there are three FCHO paralogs: neuronal enriched FCHO-1, ubiquitously expressed FCHO-2 and the neuronal specific SGIP1 (SH3-containing GRB2-like protein 3-interacting protein 1) [94-97]. In *C.elegans*, there is only one *fcho* gene, encoding for FCHO-1. Largely conserved between species, FCHO-1 harbors three key functional domains: 1) the curvature sensing F-BAR domain, which can bind and promote the bending of PMs [98], 2) the APA-domain, which binds and activates AP-2 [88], and 3) μ -homology domain which is structurally similar to the medium μ -subunit of AP2, which is recognized by many endocytic proteins and thus functions as an endocytic interaction hub [73, 94, 97, 99].

FCHO-1 is noted for its allosteric activation of AP-2 and involved in a competing model that suggests its requirement in initiating CME. In this model, it is proposed that it interacts with other early arriving endocytic proteins, collectively known as “endocytic pioneers”, to initiate and stabilize AP-2 at the PM, while simultaneously allosterically activating AP-2, ultimately initiating CME [89, 90, 97]. Similar to AP-2 ablation, the loss of FCHO-2 is postpartum lethal in mice. In humans, homozygous recessive mutations of FCHO-1 can become deadly, due to faulty CME and immunosuppression [100, 101]. In *C. elegans*, null *fcho-1* mutants are viable which offers a means to investigate associate outcomes in these mutants. This extends an avenue to examine impaired AP-2 function and to discern how FCHO-1 is essential in CME. In *C.elegans* FCHO-1 is dispensable in animals that have AP2 mutations that destabilize its closed conformation

[88, 102, 103]. Similarly, NECAP depletion results in the dwelling of AP-2 in its inactivated stage, which can be overcome by the overexpression of FCHO-1 [104]. Though disagreeing models for FCHO-1 in the initiation of CME remain, its functional relationship to AP-2 is largely agreed upon. Nevertheless, a putative role for FCHO-1 in neurons remains uncertain and is largely unexplored. This is particularly intriguing considering the enrichment of FCHO proteins in neurons, combined with the neural specificity of SGIP1 in vertebrates. If CME is important in all cells and FCHO-1 activates a central component of CME (AP-2), then why the need for a neuronal-specific enrichment of FCHO-1? This question is even more fascinating amid debates of CME/FCHO-1's role in SV recycling.

Disrupted Endocytosis: Implications for Neurodegenerative Disorders

Given the multifaceted roles of endocytosis in sustaining neuronal structure and function, it is to be expected that compromises in endocytic integrity are intricately linked to a myriad of neurological and neurodegenerative diseases. CME has been implicated in several neuronal specific diseases. Dysfunction of CME proteins, such as clathrin and several other associated proteins have been linked to various neurological conditions, including but not limited to: epilepsy [51, 105, 106], schizophrenia [107], Huntington's disease [108], Parkinson's disease [109, 110], and Alzheimer's disease [111-113]. In particular, the critical role of clathrin in synaptic vesicle reformation highlights why mutations or alterations in several well-characterized clathrin-associated proteins are linked to neurodegeneration. For instance, deficiencies in the membrane curvature sensing protein Endophilin-A (component of both CME and ultrafast endocytosis) are connected to age-dependent degeneration of the nervous system

[114]. Additionally, mutations in the phosphoinositide phosphatase, synaptojanin-1, (CME and ultrafast endocytosis), are associated with inherited forms of Parkinson's disease [115, 116]. Moreover, Alzheimer's disease has been linked to a selective reduction in the clathrin adaptors (APs) including AP-2 and the neuronal specific, AP180 [117]. The desire for a comprehensive understanding of CME has laid the groundwork for investigations aiming to establish connections between its dysregulation and the onset of neurodegenerative diseases. Albeit it is likely that future studies will continue to emerge linking additional endocytic pathways and neuronal disorders, once those pathways are better understood.

CHAPTER 4: Key Findings in Dissertation Research

In my dissertation research, I took a forward genetic approach to identify and subsequently investigate additional endocytic pathways that support synaptic function in *C.elegans* neurons. Towards this goal, I executed experiments that bred five major takeaways. **1)** I first identified the endocytic protein FCHO-1 in a randomized forward genetic screen performed in Endophilin/*unc-57* mutants, in search of viable mutations that exacerbated synaptic dysfunction. This suggested that an endocytic pathway involving FCHO-1 complements a distinct Endophilin/UNC-57 dependent pathway in supporting neuronal function. **2)** I next performed locomotion assays and electrophysiology experiments, which confirmed that synaptic function was negatively impacted and additive in *unc-57; fcho-1* double mutants and significantly impeded in singular *fcho-1* mutants in comparison to their wild-type counterparts. **3)** With the use of electron-microscopy, we discovered that SV morphology and dynamics are differentially altered in individual Endophilin/*unc-57* and *fcho-1* mutants. Notably, Endophilin/*unc-57* mutants uniquely displayed a severe depletion of SVs at neuronal synapses which did not occur in *fcho-1* mutants, but instead displayed intriguing “breaks” along neuronal membranes. **4)** Proceeding the developed of an *in vivo* system, coined PAGEN, we found an increased exchange of cellular content between distinct neuronal types in *fcho-1* mutants. **5)** Alas, we demonstrated that the preservation of cellular boundaries is likely guided by an AP-2 mediated pathway, and propose these breaks are the consequence of an accumulation of the neuronal enriched CAM protein, SYG-1, whose endocytosis is likely halted in the absence of FCHO-1. These experiments, and their results, are described in greater detail in chapter 5 of this dissertation.

CHAPTER 5:

FCHO-1 Functions Through an AP-2 Mediated Pathway That is Necessary to Maintain the Structural Integrity of Neuronal Membranes

INTRODUCTION

Neurons rely on a diverse array of membrane trafficking pathways to support their essential functions and protect their viability. Due to the post-mitotic nature of neurons and the rapid rates at which they must perform, these pathways must function indefinitely with precision and speed to meet the unique and continuous demands of neuronal activity. Endocytosis is a critical membrane trafficking pathway, playing an essential role in a myriad of neuronal functions, beyond those sustain cellular homeostasis. Of note, these functions include regulating cell adhesion in support of the stability and plasticity of neuronal circuits and the recycling of synaptic vesicles (SVs) to maintain synaptic transmission [19, 20, 25, 28]. To accommodate these various tasks, several kinetically distinct endocytic pathways exist that utilize varying combinations of exclusive and shared proteins. These endocytic pathways collectively contribute to maintaining the delicate balance of membrane composition and ultimately the integrity of neurons. Disruption of any of these programs can lead to synaptic dysfunction, impaired neuronal communication, and often contributes to neurodegenerative diseases and disorders[107-109, 111, 112, 118]. Despite our breadth of knowledge about endocytosis programs, a comprehensive understanding of all the endocytic pathways and how they manage to sustain neurons over the course of an organism's lifetime is still lacking.

The major endocytic program for membrane cargo internalization is clathrin-mediated endocytosis (CME). In neurons, CME occurs at several distinct regions within neurons targeting a diverse array of membrane cargo in distinctive neuronal regulation programs[2, 3, 17, 34, 48, 87]. Despite CME being widely accepted as major route of

endocytosis in neurons, there remains some reservation that the kinetics of CME, ~10–30 s, is too slow to meet the demands of synaptic transmission, specifically the recycling of synaptic vesicles. Synaptic transmission is the mode of communication between neurons, wherein neurotransmitter-filled synaptic vesicles (SVs) fuse with the membranes of pre-synaptic cells in order to release their contents for retrieval by post-synaptic targets. The membranous SV proteins are instantaneously retrieved via endocytosis to swiftly reconstitute SVs, a process known as SV recycling[26]. Several studies have demonstrated that CME is necessary for SV recycling[43, 119], however additional models such as “kiss-and-run”, activity-dependent bulk endocytosis (ADBE), and ultrafast endocytosis have recently emerged [28, 54, 55, 60]. These endocytic routes are notably rapid endocytic programs that can retrieve large spans of the membrane in roughly ~1-2s and as quickly as ~50ms. It has been implicated that all four of these mechanisms may coexist at pre-synaptic terminals and have evolved to accommodate the variance of stimulus intensity, sensitivity to temperature, and type of synapse [28, 29, 63]. Interestingly, these diverse endocytic pathways often utilize the same molecular players, which has made it challenging to disentangle which endocytic pathways are uniquely engaged for a distinct task at the synapse. Additionally, these shared proteins are simultaneously participating in distinct endocytic pathways outside of the synapse, further limiting our comprehensive understanding of the functional scope of individual endocytic players within specific endocytic events, and more broadly, how these shared endocytic players are harmoniously regulated and coordinated among these varying endocytic pathways.

A key molecular component unique to CME, is the evolutionarily conserved adaptor protein 2 (AP-2) complex, crucial for sorting protein cargos into clathrin-coated vesicles [86, 87, 89, 93]. AP-2 is a heterotetrameric complex consisting of four subunits (α , β 2, μ 2, and σ 2) which toggles between a functionally active ("open") and inactive ("closed") state [88, 90, 91]. AP-2's transition between states is regulated by the endocytic protein, FCHO-1 (Fer/CIP4 Homology domain only), which binds to inactive AP-2, allosterically activating it and promoting endocytic progression [88]. Removal of FCHO-1 locks AP-2 complexes in an inactive state, preventing interaction with endocytic accessory proteins, ultimately stalling endocytosis [88, 103]. FCHO proteins are evolutionarily conserved endocytic proteins belonging to the muniscins family. In mammals, there are three FCHO paralogs: FCHO-1 which is predominantly expressed in neuronal and lymphoid cells, FCHO-2 [95, 98, 120] which is ubiquitously expressed, and SGIP1, whose expression is thought to be restricted to neuronal tissues [121]. In *C.elegans* there is only one FCHO-1 protein encoded by a single gene, *fcho-1*, and harbors three key functional domains that are largely similar to its mammalian orthologues: 1) the curvature sensing F-BAR domain, which can bind and promote the bending of PMs [97], 2) the APA-domain, which binds and activates AP-2 [88] and 3) μ -homology domain akin to the medium subunit of AP2, which is recognized by many endocytic proteins and thus functions as an endocytic interaction hub [73, 94, 99]. To date, the majority of studies on FCHO-1 and AP-2 have focused on their endocytic role in non-neuronal cells [89, 97, 103]; whereby a putative neuronal function of FCHO-1 remains largely unknown.

Other seminal endocytic proteins including Endophilin, synaptojanin, dynamin-1, as well as polymerized actin are also essential for CME[29, 49] . On the contrary, unlike AP-2, and presumably FCHO-1, these endocytic proteins are also key molecular players in ultrafast endocytosis[63] in addition to other clathrin-independent endocytic routes[122, 123]. Endophilin and synaptojanin work synergically coordinate the tubulation of the invaginated membrane, which forms the neck of the budding vesicle during endocytosis. Dynamin-1, a large GTPase, then cleaves the budding vesicle at the newly formed neck to complete endocytic internalization. Mutant animals lacking either Endophilin or synaptojanin similarly result in a severe depletion of synaptic vesicles and ultimately a failure in synaptic transmission [124]. However, despite these detrimental consequences, the mutants are viable and remarkably, residual synaptic activity persists. This is indicative that other endocytic pathways must still be active to support synaptic transmission in parallel pathways that do not require Endophilin activity yet complement optimal synaptic transmission.

To identify these additional endocytic pathways, we performed a genetic screen in Endophilin mutants (UNC-57 in *C.elegans*) to identify candidate molecules that further exacerbates the synaptic defects found in Endophilin mutants. In this study our results implicate a pathway for regulating the structural integrity of neurons in which FCHO-1 and AP-2 are key players and where Endophilin/UNC-57 is likely dispensable.

RESULTS

***fcho-1* mutations exacerbate physiological impairments in Endophilin null mutant worms.**

To investigate the mechanisms that maintain animal physiology in the absence of Endophilin, we conducted a forward genetic screen using *Endophilin unc-57(e406) null* mutant worms to identify mutations that further compromise brood size and locomotion. We found a mutant strain, BJH2250, which exhibited significantly reduced brood size, slowed locomotion (**Figure S1**), and a "jowls" phenotype previously reported in mutant worms with defective AP2-dependent pathways [88, 125]. Our sequencing results showed that the BJH2250 strain carries a 25nt deletion (**Figure S1a**) eliminating the start codon of *fcho-1*, a gene encoding the Fer/CIP4 Homology domain-only (FCHO) protein, FCHO-1, in *C. elegans*. Given the critical role of FCHO-1 in activating the AP2 adaptor complexes [88, 125, 126], we next examined the impact of *fcho-1* mutants on animal physiology in *C. elegans*.

We recreated the 25nt deletion allele (*pek230*) in *fcho-1* using CRISPR-Cas9 and homologous recombination, and subsequently conducted three functional assays to assess the effect of the *fcho-1(pek230)* mutation on *endophilin/unc-57* mutant animals. First, we compared the progeny numbers produced by *unc-57(e406); fcho-1(pek230)* double mutants to those generated by *unc-57(e406)* single mutants. The *unc-57* single mutant worms produced ~195 F1 worms each, while *unc-57; fcho-1* double mutant worms only produced ~70 F1s (**Figure S1b**). These findings indicate that *fcho-1* removal substantially reduces the brood size of *unc-57* mutants.

Second, we performed an exploration assay to evaluate the impact of *fcho-1(pek230)* on locomotion in *unc-57* mutant worms. By examining the tracks left by individual animals on the bacterial lawn and counting the number of squares on the plates covered by the worm tracks (**Figure 1A, Left**), we determined the area of the plate the worms had explored. For a period of 17 hours, *unc-57; fcho-1* double mutants covered only ~7% of the plate area (~17 squares), whereas *unc-57* single mutants covered ~10% of the plate area (~24 squares) (**Figure 1A, Right**). These results demonstrated that *fcho-1(pek230)* further impairs locomotory rates in worms lacking Endophilin/UNC-57.

Third, we assessed synaptic transmission levels at neuromuscular junctions in *unc-57; fcho-1* double mutants and *unc-57* single mutants through electrophysiological recordings. Our findings revealed that the amplitude of evoked excitatory postsynaptic currents (evoked EPSCs) in *unc-57; fcho-1* double mutants was significantly lower than in *unc-57* single mutants (0.5 ± 0.1 nA vs. 1.0 ± 0.1 nA, respectively) (**Figure 1B**), suggesting an additive role for FCHO-1 in evoked synaptic responses in the absence of Endophilin/UNC-57. However, *fcho-1(pek230)* did not significantly affect endogenous EPSCs in *unc-57* mutant worms, as the rate and amplitude of endogenous EPSCs in *unc-57; fcho-1* double mutants were similar to *unc-57* single mutants (**Figure 1C**). Nonetheless, the reduced evoked EPSC responses in *unc-57; fcho-1* double mutants reveal a role for FCHO-1 that is independent of Endophilin in synaptic transmission.

Collectively, results from the three assays demonstrate that FCHO-1 disruption leads to additive defects in animal physiology in *Endophilin/unc-57* mutant animals,

indicating that FCHO-1 has distinct roles from Endophilin, despite both being endocytic proteins.

***fcho-1* single mutant animals show physiological defects.**

To determine the role of FCHO-1 in animal physiology, we next quantified locomotion rates and excitatory postsynaptic currents in *fcho-1(pek230)* single mutant worms. We found that *fcho-1* mutant animals moved more slowly than wild-type animals (Figure 2A; *fcho-1* mutants $\sim 122 \pm 4$ $\mu\text{m/s}$, and wild-type $\sim 156 \pm 3$ $\mu\text{m/s}$, respectively), indicating that *fcho-1* supports normal locomotion in *C. elegans*. Subsequently, we monitored synaptic transmission at neuromuscular junctions in *fcho-1(pek230)* mutant worms by electrophysiological recordings. We observed that evoked EPSC amplitudes were significantly reduced in *fcho-1* mutants (**Figure 2B**), suggesting a supportive role of FCHO-1 in synaptic transmission in response to stimulation.

It is worth noting that animals carrying individual *fcho-1* or *Endophilin unc-57* mutations exhibited distinct physiological changes. First, the defects in locomotory rates and evoked EPSC amplitudes observed in *fcho-1* single mutant worms were considerably less severe than those observed in *Endophilin unc-57* single mutant worms[64] (**Figure 1B**). Second, disruption of *unc-57* led to a strong reduction in the frequency of endogenous EPSCs, which was not observed in *fcho-1* single mutant worms. Coupled with our identification of *fcho-1(pek230)* from an enhancement screen of *Endophilin/unc-57* mutants, the observed variations in how the singular mutants alter animal physiology, strongly suggests that Endophilin and FCHO-1 have distinct roles *in vivo*.

FCHO-1 functions in neurons to support locomotion and synaptic transmission.

To investigate where FCHO-1 acts to support animal physiology, we conducted tissue-specific rescue experiments on *fcho-1(pek230)* single mutant animals. We found that a single-copy transgene expressing GFP-tagged FCHO-1 (GFP::FCHO-1) in neurons under a pan-neuronal promoter (*snb-1p*) fully restored the locomotory rates (**Figure 2A**) and evoked EPSC amplitudes (**Figure 2B**) of *fcho-1* mutants back to wild-type levels, indicating a neuronal role for *fcho-1*. In contrast, GFP::FCHO-1 expression in muscles, driven by the myosin promoter (*unc-54p*), failed to recover locomotion rates and evoked EPSC amplitudes in *fcho-1* mutants (**Figure 2**). These results demonstrate that FCHO-1 has a neuronal function in maintaining normal locomotion and synaptic transmission *in vivo*.

Synaptic vesicle endocytosis remains normal in *fcho-1* mutants.

Since FCHO-1 has an endocytic role in non-neuronal cells, we examined the impact of FCHO-1 disruption on synaptic vesicle endocytosis in living neurons using an established fluorescence imaging assay[127, 128]. Briefly, a pH-sensitive GFP, pHluorin, was inserted into the first luminal domain of the vesicular glutamate transporter EAT-4 (VGLUT). In the absence of stimuli, the VGLUT-pHluorin remains in the lumen of synaptic vesicles, and the green fluorescence of pHluorin is quenched due to the acidic pH of the vesicle lumen. Upon stimulation, synaptic vesicles undergo exocytosis, and the VGLUT-pHluorin is delivered to the plasma membrane, exposed to the neutral extracellular pH, enhancing the green fluorescence of pHluorin. Subsequent endocytosis of synaptic vesicles returns VGLUT-pHluorin back inside the acidic lumen,

quenching the visible fluorescence signal. Changes in synaptic vesicle endocytosis can be evaluated by following the return of VGLUT-pHluorin fluorescence to its quenched state after stimulation. Surprisingly, *fcho-1* mutants exhibited normal rates of VGLUT-pHluorin retrieval, identical to those in wild type animals (**Figure 3A and 3C**). In contrast, the rate of VGLUT-pHluorin retrieval in Endophilin/*unc-57* mutants was significantly slower than that in wild type animals, suggesting further that Endophilin and FCHO-1 differentially support neuronal function at synapses.

Synapses in *fcho-1* mutants display morphological changes at ultrastructural levels

Next, we performed transmission electron microscopy to analyze the ultrastructural morphology of *fcho-1* mutant synapses, which were cryofixed using high-pressure freezing and freeze-substitution. Our analysis identified several changes. First, the abundance of synaptic vesicles at *fcho-1* mutant synapses was slightly but significantly reduced, from 39 ± 2 vesicles per synaptic profile in wild type animals to 31 ± 3 vesicles at *fcho-1* mutant synapses (**Figure 4A**). In contrast to the minor changes at *fcho-1* mutant synapses, the abundance of synaptic vesicles at *Endophilin/unc-57* mutant synapses decreased to only 16 ± 1 per synaptic profile, which likely corresponds to the severe decline in synaptic transmission at synapses lacking Endophilin, reported in Figure 1.

Second, we found that the average size of synaptic vesicles became larger at *fcho-1* mutant synapses (37 ± 1 nm at *fcho-1* synapses versus 33 ± 1 nm at wild type synapses); however, the size of synaptic vesicles at *Endophilin/unc-57* mutant synapses remained at ~ 33 nm in diameter (**Figure 4B**). It is worth noting that the

amplitudes of endogenous EPSCs at *fcho-1* synapses were statistically identical to those at wild type synapses, suggesting that defects in synaptic vesicle diameter at *fcho-1* synapses could be too small to be reliably detected by electrophysiological recordings.

Lastly, we observed that in *fcho-1* mutant worms, many abnormal breaks occurred predominantly at contact sites between neighboring neurons (**Figure 4C**). We quantified the occurrence of these abnormal breaks in individual electron microscopy micrographs by calculating the ratio between the number of breaks and the number of neurons in the ventral nerve cord. Our data showed that the fraction of abnormal breaks in *fcho-1* mutant neurons reached ~ 0.5 , which was drastically higher than that seen in wild type neurons (~ 0.1). Although *Endophilin/unc-57* mutant neurons exhibited more severe defects in synaptic transmission and synaptic vesicle abundance compared to *fcho-1* mutants, the fraction of abnormal breaks observed in neurons lacking *Endophilin/unc-57* only slightly increased to ~ 0.2 compared to wild type neurons and was significantly lower than that seen in *fcho-1* mutants (~ 0.5). The frequent appearance of abnormal breaks in *fcho-1* mutant neurons suggests that neuron-neuron boundaries in these neurons are likely fragile and compromised, unable to withstand mechanical challenges during cryofixation. This raises the possibility of defective integrity of neuronal boundaries in neurons lacking FCHO-1.

Enhanced cellular content exchange among neurons in *fcho-1* mutant worms

Upon observing disruptions in neuronal boundaries in *fcho-1* mutant worms, we investigated the potential for abnormal cellular content exchange between distinct neuron classes. To explore this, we developed a Protease Assisted GFP Expression

(PAGEN) assay using the *quas*-QF binary expression system[129]. The PAGEN assay involves attaching the QF transcription factor to the cytoplasmic end of the integral plasma membrane protein UNC-64 (UNC-64::QF), which inhibits QF from entering the nucleus and activating GFP expression via the *quas* enhancer. We incorporated cleavage sites for the TEV protease and a nanobody targeting sequence into the linker connecting QF and UNC-64. This design enables the liberation of QF from the plasma membrane when TEV proteases are expressed. Without the TEV protease, expressing UNC-64::QF alone in cholinergic neurons (controlled by the *unc-17* promoter *unc-17p*) resulted in no GFP expression (**Figure 5A, Left**). However, co-expression of UNC-64::QF and nanobody-tethered TEV protease in cholinergic neurons led to strong GFP expression in all cholinergic neurons (**Supplemental, Figure S2**) indicating that TEV proteases liberated QF from the plasma membrane anchors and activated GFP expression after entering the nucleus.

To assess cellular content exchange between neighboring neurons, we expressed UNC-64::QF in cholinergic neurons using the *unc-17p* promoter and nanobody-tethered TEV proteases in dopaminergic neurons, driven by the *dat-1* promoter (*dat-1p*). Although neurites of dopaminergic and cholinergic neurons run together in the nerve ring and ventral nerve cord in *C. elegans*, cellular components in these neurons should be physically separated when neuronal boundaries are intact. As expected, most wild type animals expressing UNC-64::QF in cholinergic neurons and nanobody-tethered TEV proteases in dopaminergic neurons showed no green fluorescence (**Figure 5B-C**). A small fraction of wild type worms (~29%, n=163) displayed faint GFP fluorescence in one or a few neuronal cell bodies (**Figure 5B-C**), suggesting a low level of cellular

content exchange can occur between dopaminergic and cholinergic neurons in wild type conditions, possibly due to mild neuronal injuries from normal physical activities. However, we consistently found that more than half of *fcho-1* mutant animals observed (~58%, n=175) expressed GFP which did not occur in wild type animals (**Figure 5B-C**). Though we found it difficult to quantify, it is worth mentioning that GFP fluorescence in *fcho-1* mutant worms was strong and frequently appeared in more than two neuronal cell bodies and neurites. Though some wild-type animals did express GFP in several neurons, GFP expression was typically restricted to one or two neurites in the large majority (**Figure 5D**). The impact of FCHO-1 on neuronal boundaries appears to be specific, as the removal of Endophilin/UNC-57 showed a reduced, albeit not statistically significant, trend in the fraction of worms carrying GFP fluorescence compared to wild type worms (**Figure 5C**). These results indicate an increased likelihood of cellular content sharing among neurons in *fcho-1* mutant worms, supporting the notion that neuronal boundaries are compromised in the absence of FCHO-1. Moreover, these data implicate a molecular pathway that supports the integrity of boundaries, that is not perturbed by loss of Endophilin/UNC-57, but where FCHO-1 activity is necessary.

Accumulation of the cell adhesion protein SYG-1 in *fcho-1* mutant neurons.

In electron microscopy analysis, we observed that breaks in *fcho-1* mutant neurons often occurred at electron-dense regions (**Figure 4A**) which resemble neuron-neuron contact sites enriched with adhesion molecules. This observation prompted us to investigate the hypothesis that adhesion molecules may abnormally accumulate in neurons lacking FCHO-1. To examine this model, we studied the impact of FCHO-1 removal on the abundance of SYG-1 in neurons. SYG-1, an evolutionarily conserved

multipurpose cell adhesion molecule, belongs to the immunoglobulin superfamily. It is required for neurite placement[130] and synaptogenesis[131, 132] due to its ability to modulate adhesive forces via local F-actin rearrangements[133]and recruit synaptic protein partners[134].

To determine the abundance and distribution of SYG-1, we generated a single-copy transgene that expressed GFP-tagged SYG-1 (SYG-1::GFP) in cholinergic DB neurons using the *unc-129p* promoter[135]. Our imaging analysis (**Figure 6A**) revealed that, compared to wild type neurons, SYG-1::GFP in *fcho-1* mutants exhibited a significant increase in the peak intensity value of fluorescent puncta (**Figure 6B**) and axonal fluorescence (**Figure 6C**), indicating an accumulation of SYG-1::GFP in *fcho-1* mutant neurons. In contrast, no significant changes were observed in the width (**Figure 6D**) or density (**Figure 6E**) of SYG-1::GFP puncta, suggesting that the overall development of synapses was not disrupted in neurons lacking FCHO-1. Together, these data indicate that FCHO-1 removal increases the abundance of the adhesion protein SYG-1 in neurons.

FCHO-1 colocalizes with AP-2, but not Endophilin, at the synapses.

Neurons exhibit multiple endocytic pathways. FCHO-1 functions as an allosteric activator of the adaptor complex 2 (AP-2), wherein it binds to and induces a conformational change in AP-2, facilitating clathrin-dependent endocytosis of cargo proteins[88, 90]. In contrast, Endophilin/UNC-57 functions in both clathrin-independent and clathrin-dependent endocytosis in neuronal and non-neuronal cells [64, 122-124, 136-139]. To depict a pathway for FCHO-1 in neurons, we examined its distribution in axons using fluorescence microscopy with respect to AP-2 and Endophilin/UNC-57.

We generated a single-copy transgene expressing TagRFP::FCHO-1 in cholinergic DB neurons under the control of the *unc-129p* promoter (**Supplementary Figure S4**). The red fluorescent protein-tagged FCHO-1 enabled us to visualize its distribution within neurons. We found that TagRFP::FCHO-1 colocalized with GFP-tagged AP-2 subunits, α -adaptin (APA-2::GFP) and mu-2 subunit (APM-2::GFP), in synaptic fluorescent puncta along the dorsal axons of DB neurons (**Figure 7A**). Conversely, Endophilin UNC-57::GFP did not colocalize with TagRFP::FCHO-1, even though both proteins were enriched in the same synapses. These findings suggest that FCHO-1 and Endophilin/UNC-57 predominantly occupy distinct subsynaptic locations within neurons.

FIGURES

Figure 1 Jimenez et al.

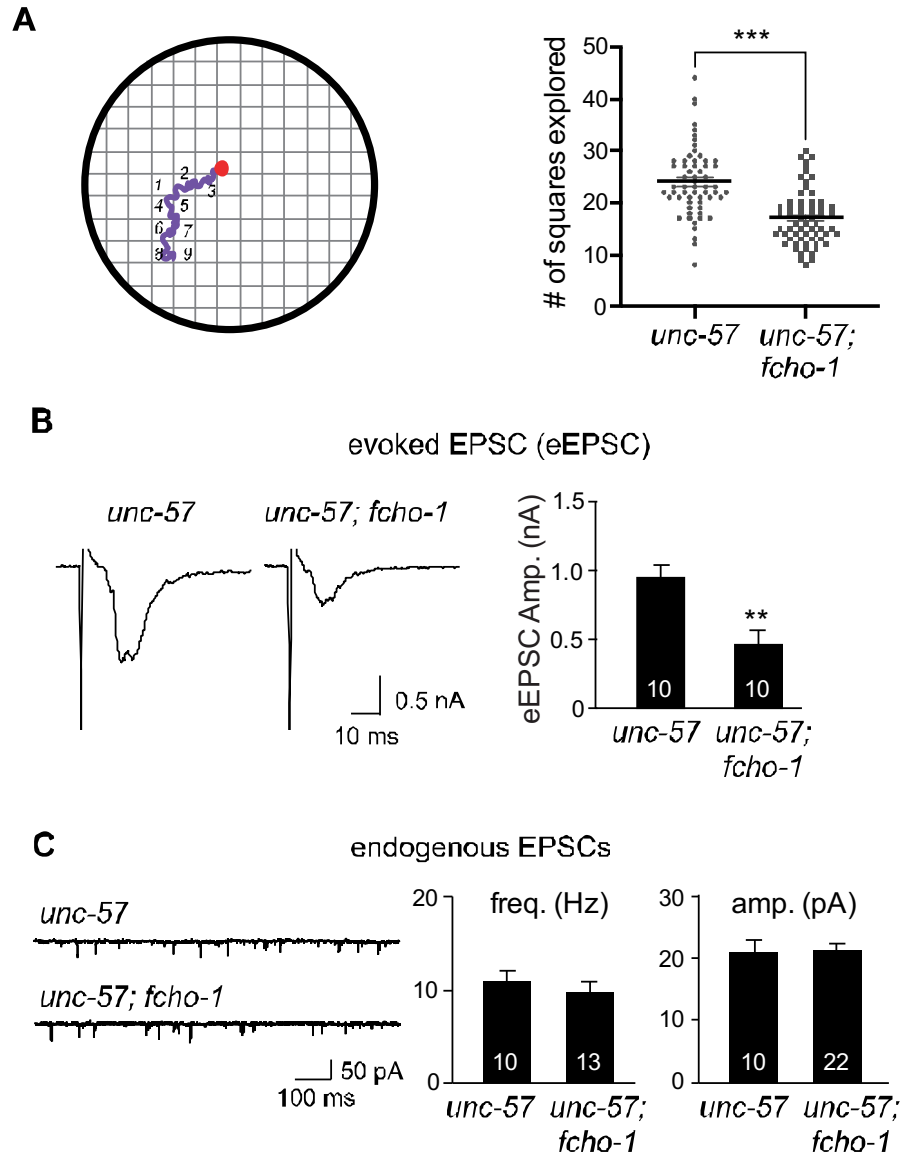


Figure 2. Deletion of *fcho-1* exacerbates locomotory and synaptic defects in

***Endophilin null* mutant worms. (A) (Left)** A schematic depicting the exploration assay.

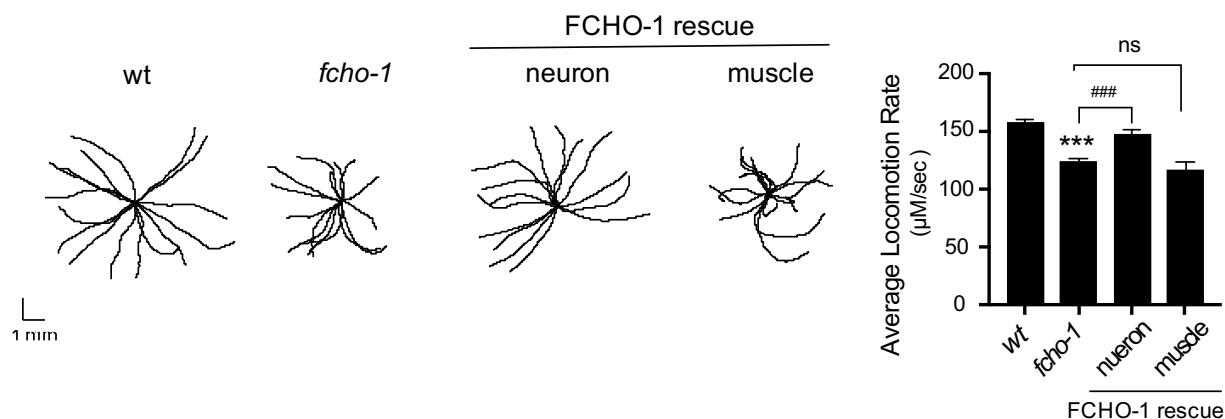
The red dot indicates where the worm was placed at the beginning of the assay, and the

purple line indicates the track left on the NGM plate by a singular animal over 17 hours.

(Right) The exploration capacities of age-matched *unc-57* single mutant and *unc-57; fcho-1* double mutant animals were compared by quantifying the number of squares explored by the worms. Each data point represents the number of squares explored by a single animal (mean \pm SEM; *unc-57*: 24 ± 1 , n=60, *unc-57; fcho-1*: 17 ± 1 , n=63). **(B-C)** Excitatory postsynaptic currents (EPSCs) were measured by electrophysiological recordings at neuromuscular junctions in *unc-57* single mutant and *unc-57; fcho-1* double mutant worms. **(B)** Representative traces of evoked EPSCs (*left*) and summary data for evoked EPSC amplitude (*right*; *unc-57; fcho-1* double mutants: 0.5 ± 0.1 nA; *unc-57* single mutants: 1.0 ± 0.1 nA) are shown. **(C)** Representative traces of endogenous EPSCs (*left*), summary data for the rates of endogenous EPSCs (*middle*), and amplitude of endogenous EPSCs (*right*) are shown. The number of animals analyzed for each genotype is indicated in the bar graphs. ***, $p < 0.001$ and **, $p < 0.01$ when compared to *unc-57* single mutants; statistics were performed using unpaired t-test. Error bars represent standard error of the mean (SEM).

Figure 2 Jimenez et al.

A.



B.

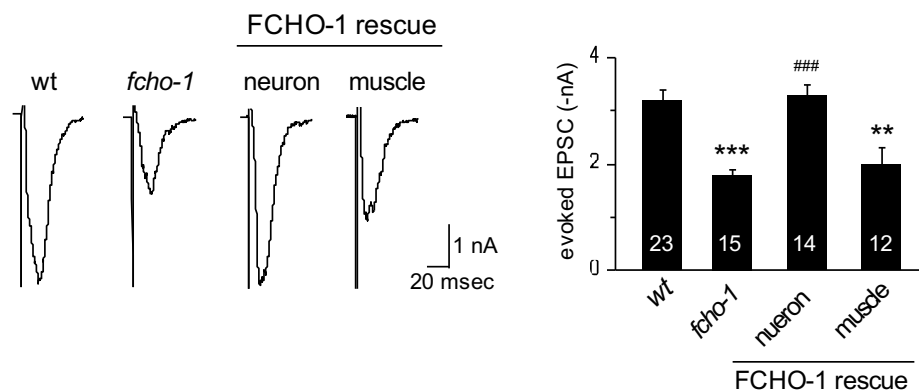


Figure 2. Neuronal expression of FCHO-1 restores locomotion and synaptic

transmission in *fcho-1* mutant animals. Wild type N2 and *fcho-1*(*pek230*) mutant

worms were used for locomotion analysis and electrophysiological recordings. Single-

copy transgene introduced to express GFP-tagged FCHO-1 in neurons and expressed

ectopically in muscles (“neuron” indicates *snb-1p::gfp::fcho-1*, and “muscle” indicates

unc-54p::gfp::fcho-1) in *fcho-1*(*pek230*) mutant worms. **(A)** Representative traces of

locomotion trajectories during a 30-second time frame are shown (n=15 for each

respective genotype) in the *left* panels. Quantification of locomotion rates is plotted for

each indicated genotype in the *right* panel (mean \pm SEM: $157 \pm 3 \mu\text{M/s}$, $n=159$ for wild type; $122 \pm 4 \mu\text{M/s}$, $n=126$ for *fcho-1* mutant worms; $147 \pm 5 \mu\text{M/s}$, $n=99$ for neuron expression of GFP::*FCHO-1*; and $117 \pm 6 \mu\text{M/s}$, $n=40$ for muscle expression of GFP::*FCHO-1*). ***, $p < 0.001$ when compared to wild type worms, and ####, $p < 0.001$ when compared to *fcho-1* mutant animals. **(B)** Representative traces of evoked EPSCs (*left*) and summary data of the amplitude of evoked EPSCs (*right*) are shown. The number of animals tested is indicated in the bar graph. Error bars represent standard error of the mean (SEM). ***, $p < 0.001$; **, $p < 0.01$, when compared to wild type worms, and ####, $p < 0.001$ when compared to *fcho-1* mutant animals. One-way ANOVA followed by Dunnett's multiple comparisons test was used for statistical analysis in (A) and (B).

Figure 3 Jimenez et al.

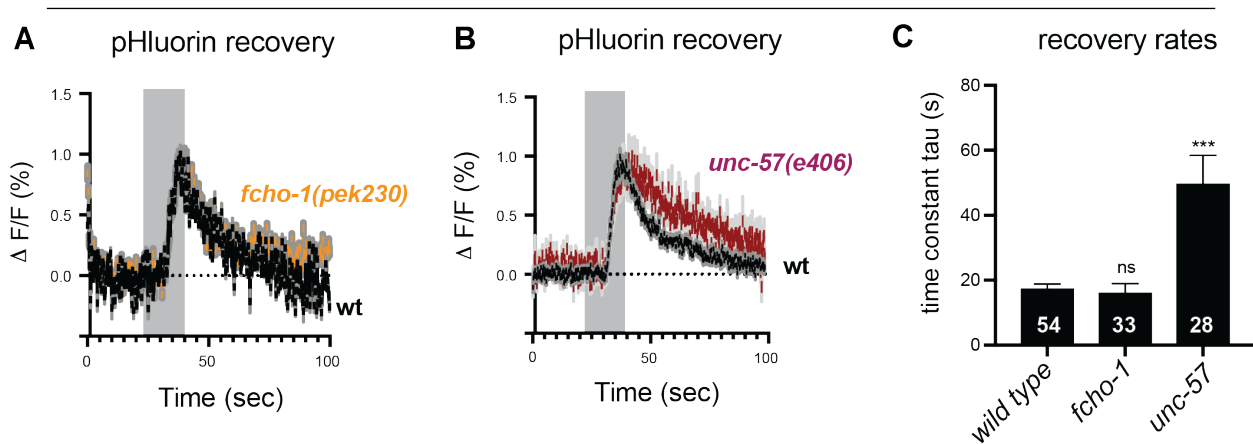


Figure 3. The rates of synaptic vesicle endocytosis remain normal in *fcho-1* mutant animals. *In vivo* fluorescence analysis to monitor the recycling of synaptic vesicle protein VGLUT-pHluorin in *C. elegans* sensory neurons (ASH) was performed

as previously described in Zhang et al., 2022[128]. Briefly, a pH-sensitive super-ecliptic pHluorin reporter was inserted into the first luminal domain of the vesicular glutamate transporter VGLUT EAT-4, designated as VGLUT-pHluorin [127]. Transgenic worms expressing VGLUT-pHluorin in the sensory ASH neuron were challenged for 10 seconds by 0.5M NaCl, which trigger synaptic vesicle exocytosis in ASH neurons, resulting in the delivery of VGLUT-pHluorin to the plasma membrane and an increase of pHluorin fluorescence. Once the stimulus is removed, the pHluorin fluorescence of VGLUT-pHluorin becomes quenched due to endocytosis and reacidification of synaptic vesicles. **(A)** Mean VGLUT-pHluorin responses from wild type (black) and *fcho-1(pek230)* mutant (orange) neurons. **(B)** Mean VGLUT-pHluorin responses from wild type (black) and *unc-57(e406)* mutant (burgundy) neurons. Gray rectangle indicates the period during which worms were exposed to NaCl stimulus. Shading on individual traces indicates SEM. **(C)** Quantification of the time constants of the recovery of VGLUT-pHluorin fluorescence. Error bars are standard error of the mean (SEM). ***, $p < 0.01$ and “ns” indicates no significance when compared to wild type worms. The number of animals tested is indicated in the bar graph.

Figure 4 Jimenez et al.

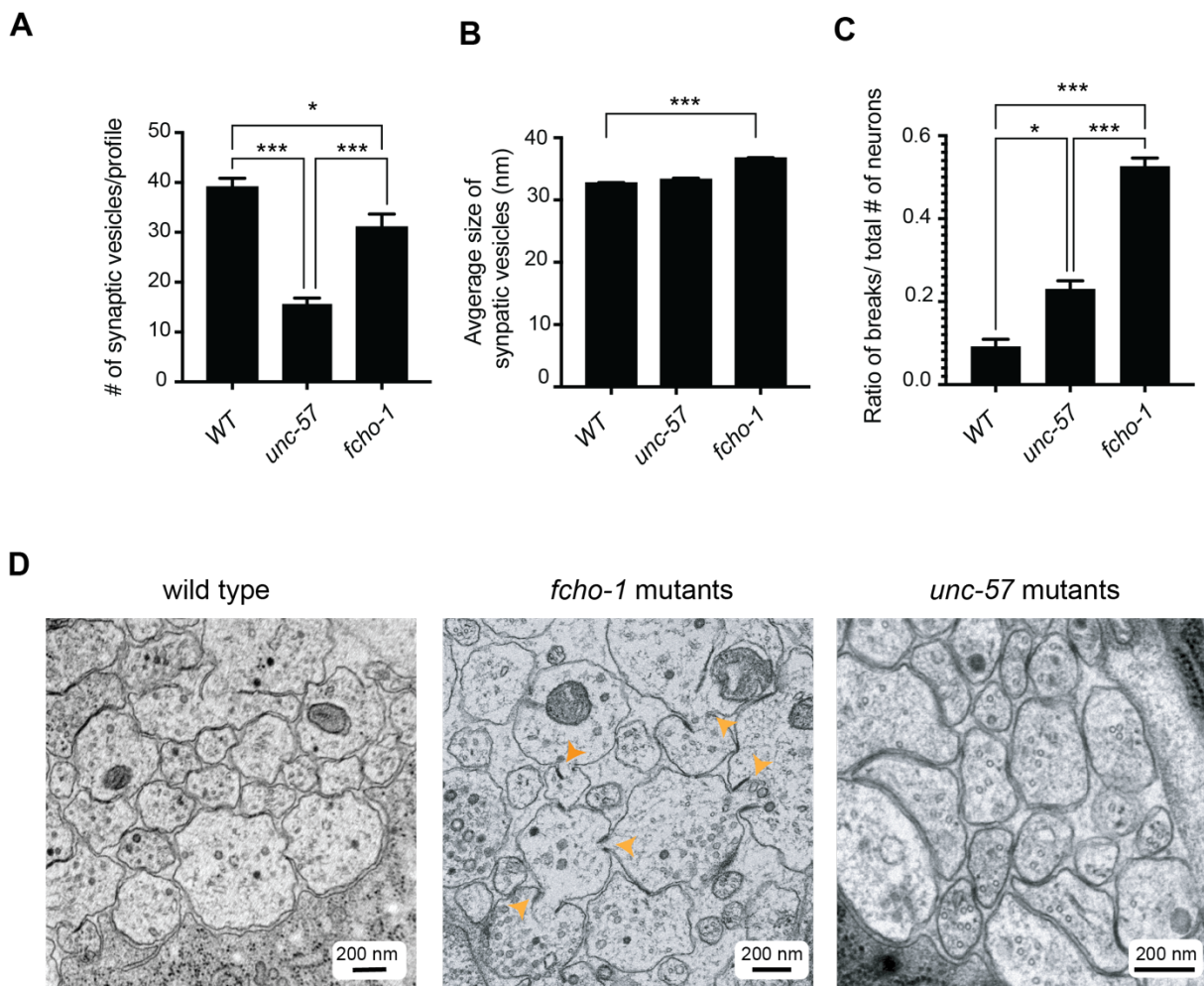


Figure 4. Ultrastructural changes in neurons lacking FCHO-1. Transmission electron microscopy was used to examine ventral nerve cords of adult hermaphrodite worms, following high-pressure freeze and freeze substitution procedures [65, 124]. **(A)** Abundance of synaptic vesicles per synaptic profile, **(B)** synaptic vesicle diameters, and **(C)** ratio of broken cellular boundaries to neurite number are presented as mean \pm standard error for each indicated genotype. **(D)** Representative transmission electron micrographs of cross-sections of adult wild type N2 (*left*), *fcho-1* mutant (*middle*), and

unc-57 mutant (*right*) ventral nerve cords at 5,000x magnification. Scale bars: 200 nm. Breaks are indicated by orange arrows. “ns” denotes no significance, ** indicates $p < 0.01$, and *** indicates $p < 0.001$ between the genotypes. Error bars represent the standard error of the mean (SEM). One-way ANOVA followed by Dunnett's test was used for statistical analyses.

Figure 5 Jimenez et al.

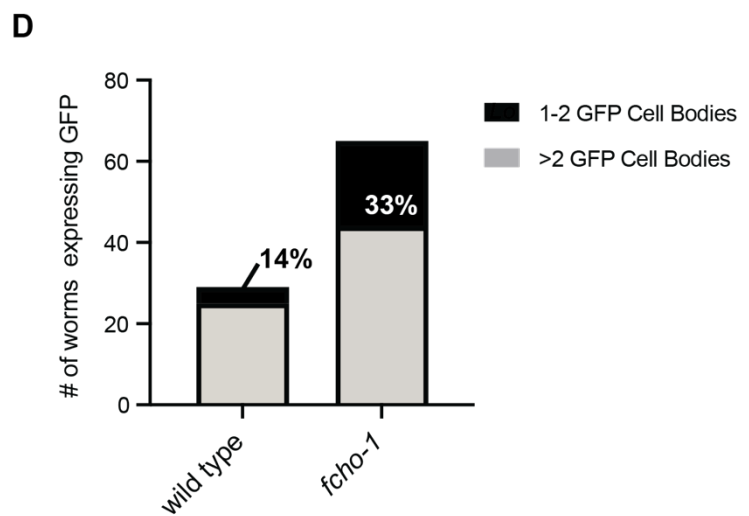
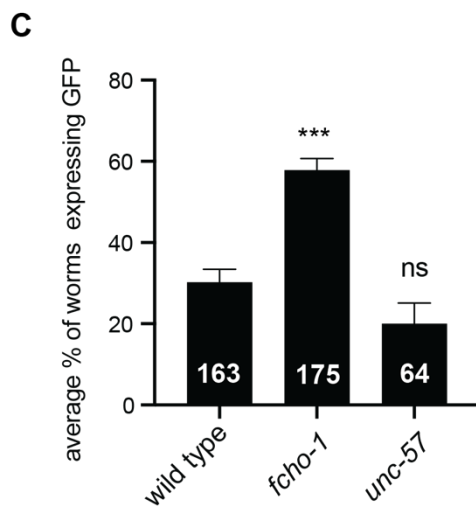
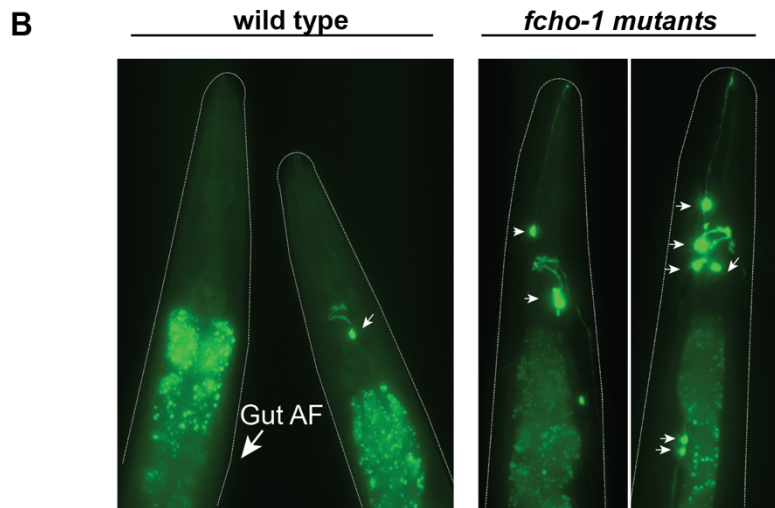
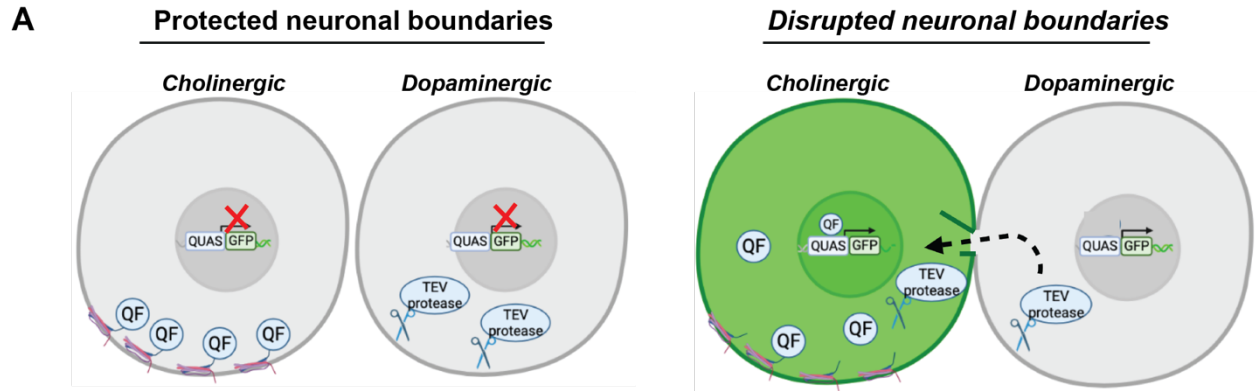


Figure 5. FCHO-1 removal results in abnormal exchange of cellular contents

between dopaminergic and cholinergic neurons. (A) Schematic of the Protease-

Assisted-Gene-Expression system (PAGEN). *(Left)* The transcription factor QF is linked to the plasma membrane protein UNC-64 (QF::UNC-64) through a peptide linker with a cleavage site for the protease TEV and an ALFA-tag sequence for single-chain

nanobody recognition [140]. QF::UNC-64, expressed in cholinergic neurons, cannot activate GFP expression via the *quas* enhancer without TEV protease, due to its

restricted plasma membrane localization. *(Right)* When breaks form between

cholinergic and dopaminergic neurons, nanobody (NbALFA)-tagged TEV proteases, expressed in dopaminergic neurons, enter cholinergic neurons. QF is subsequently

released from the plasma membrane upon proteolysis and activates GFP upon entering the nucleus of cholinergic neurons. **(B)** GFP fluorescence in wild type and *fcho-1* mutant

worms expressing the PAGEN system. Three single-copy transgenes were introduced

into worms for: 1) NbALFA-TEV expression in dopaminergic neurons by the *dat-1*

promoter, 2) QF::UNC-64 expression in cholinergic neurons by the *unc-17* promoter,

and 3) GFP expression by the *quas* enhancer. Representative images of green

fluorescence in neurons are shown for wild type *(left)* and *fcho-1* mutant worms *(right)*.

Arrows label GFP cell bodies; AF = autofluorescent gut granules. **(C)** Quantification of

the fraction of worms displaying GFP fluorescence. Mean and SEM values obtained

from four independent replicates are shown. The total number of worms examined is

indicated in each bar. ***, $p < 0.0001$; one-way ANOVA followed by Dunnett's test.

Figure 6 Jimenez et al.

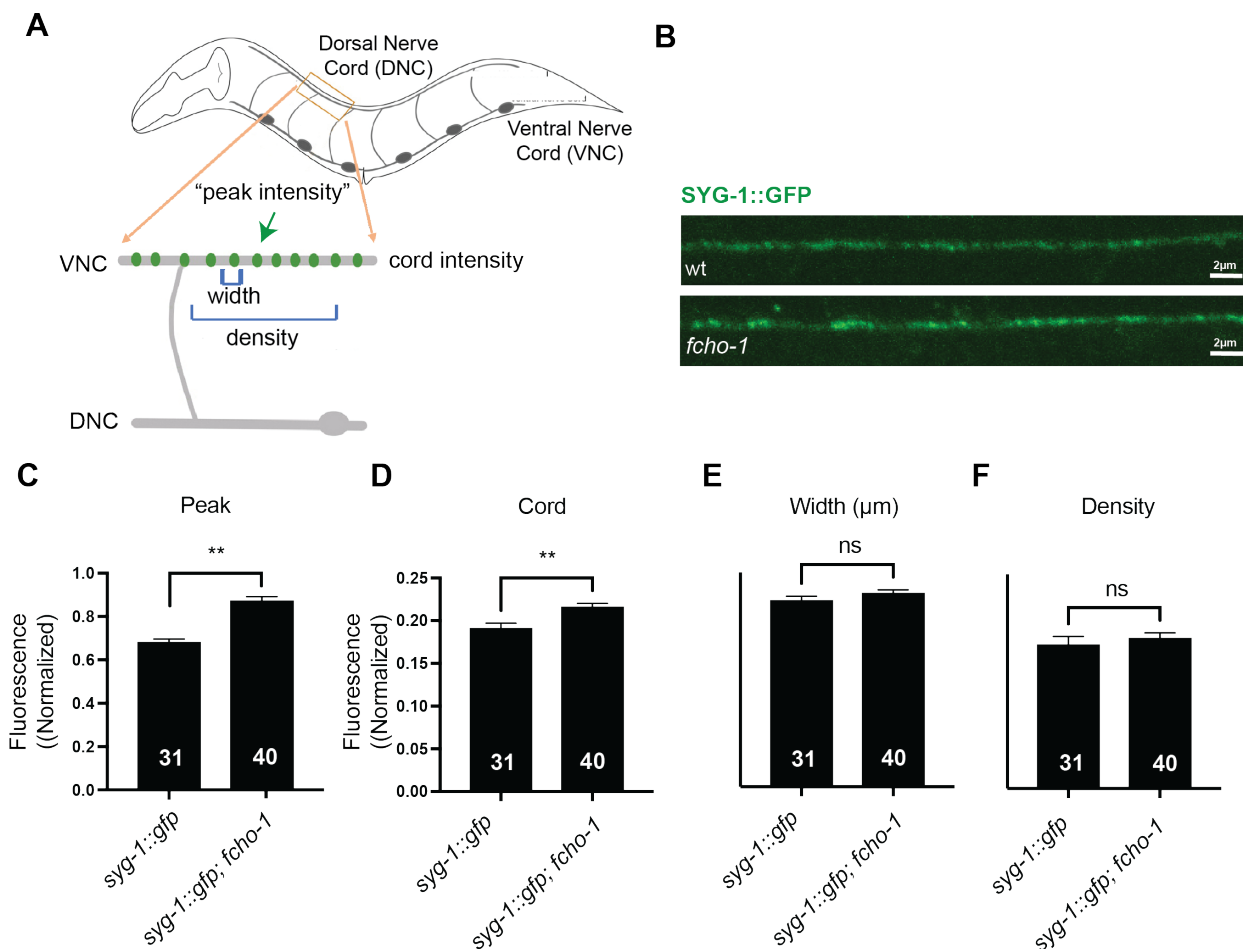


Figure 6. Deletion of *fcho-1* leads to accumulation of the adhesion protein SYG-1 in axons. GFP-tagged SYG-1 was expressed in the DB neurons using the Punc-129 promoter, through a Fluorescence intensity of SYG-1::GFP were obtained as previously described in (Dittman and Kaplan, 2006, Bai et al., 2010)[64, 119] and compared between wild type and *fcho-1* mutants. **(A)** Simplified schematic of where synaptic fluorescence was assayed and **(B)** representative images of single-copy transgene *syg-1::gfp* expression in the dorsal cord of wild type animals (Upper) and *fcho-1* mutants (Lower). Scale bar, 2 μm. **(C)** “Peak” is the absolute peak fluorescence ratio normalized to a fluorescent bead standard at individual puncta.

(D) “Cord” is the absolute axonal fluorescence (ratio of the minimum fluorescence level over a 5- μm interval over the bead standard within the dorsal cord. Data are normalized to wild type data. **(E)** “Density” is the number of peaks found per 10 μm of cord analyzed. **(F)** “Width” is the distance measured from the midpoint between the peak and baseline on either side of the peak. Widths are binned into 0.2 μm intervals and normalized to wild type data. Error bars are standard error of the mean (SEM). n=31 animals (349 synapses) for wild type and n=40 animals (471 synapses) for *fcho-1* mutants. Statistics were performed by Student’s t-test, ** indicates $p < 0.001$ compared to wild type.

Figure 7 Jimenez et al.

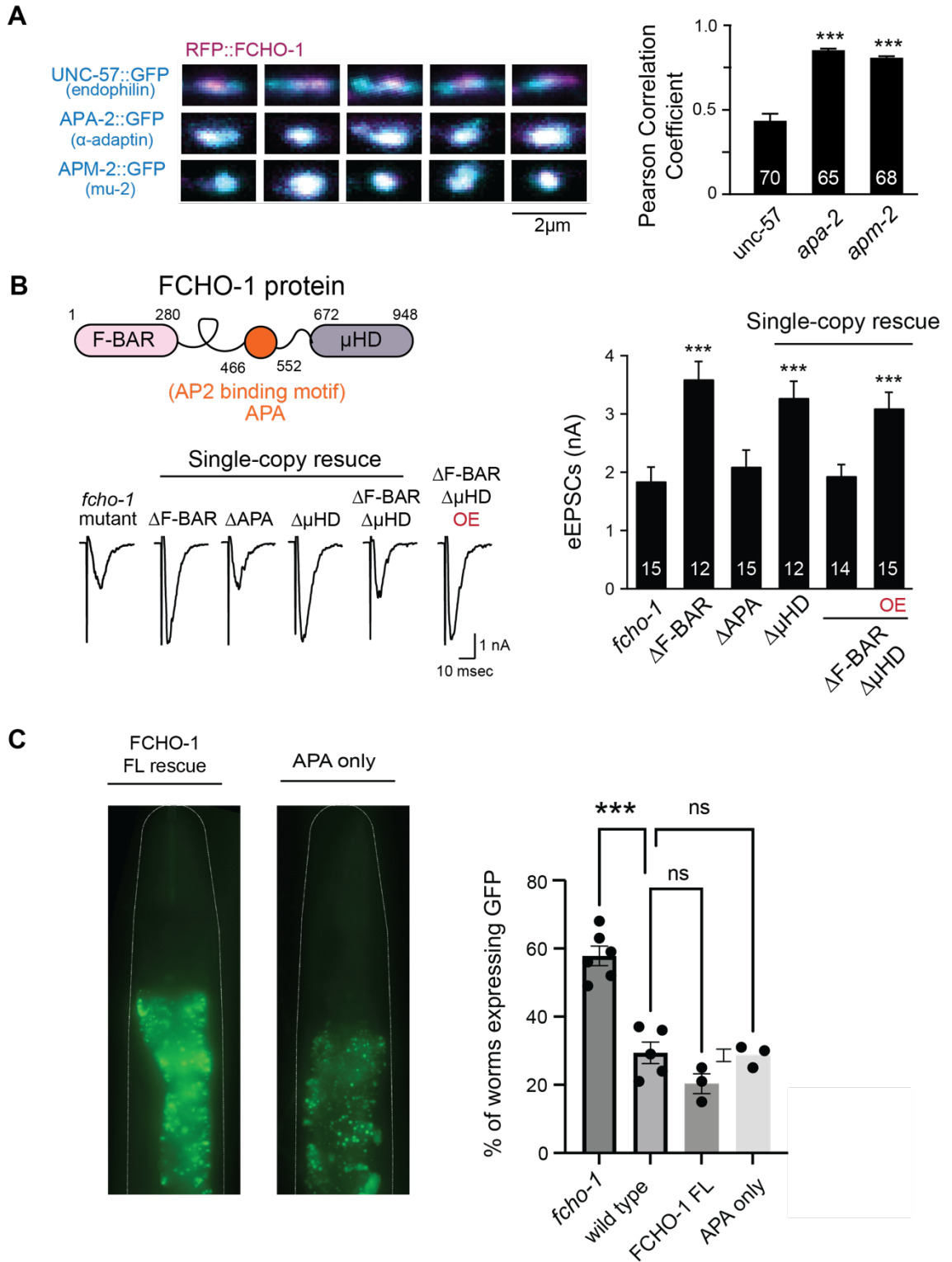


Figure 7. The AP2 binding motif of FCHO-1 is sufficient to maintain proper synaptic activity FCHO-1 does not colocalize with Endophilin (*unc-57*) but is closely associated with the AP-2 subunits, α -adaptin (*apa-2*) and mu-2 (*apm-2*) at synapses.

(A, Left) Representative images of RFP tagged FCHO-1 (mScarlet::FCHO-1), and GFP labeled Endophilin (UNC-57::mNeonGreen), α -adaptin subunit (APA-2::mNeonGreen), mu-2 subunit (APA-2::mNeonGreen) expressed in the dorsal cord. **(A, Right)** Summary data of co-localization at individual synaptic puncta are shown and were evaluated using the Pearson's Correlation Coefficient. The number of synapses analyzed for each genotype is indicated in the bar graph. *** indicates $p < 0.0001$ compared Endophilin (*unc-57*). Error bars are standard error of the mean (SEM). Student's t test was used for statistical analysis. **(B, Top)** FCHO-1 schematic demonstrating the position of the conserved motifs. Single copy transgenes were generated with deletions of the indicated motifs. **(B, Bottom)** Representative traces and summary data for evoked EPSCs (eEPSC) traces. *** indicates $p < 0.0001$ compared to *fcho-1* mutants. OE=overexpression. n number is indicated in the bar graphs. Error bars are the standard error of the mean (SEM). Student's t test was used for statistical analysis. **(C)** Representative images of FCHO-1 full length (FL) and indicated domain specific rescues via PAGEN system and respective quantification of GFP expression for each genotype is indicated on the right side of the panel. The circles in the graph denote individual replicates of ~25-30 animals on each day. The average percentage reported is the cumulative average of: worms expressing GFP/total number of worms (Mean \pm SEM: wild type: 29% \pm 3, (total: 45/163 GFP expressing animals), *fcho-1* 58% \pm 3, n= 100/175 GFP expressing animals), FCHO-1 Full Length (FL) 20% \pm 5, (total: 13/64 GFP

expressing worms), APA-only $29\% \pm 5$ (total: 20/117 GFP expressing worms). **

indicates $p < 0.001$ compared to *fcho-1* mutants; one-way ANOVA followed by Dunnett's test. Error bars are standard error of the mean (SEM).

DISCUSSION

Our studies examined the role of the endocytic protein, FCHO-1, in supporting neuronal function in *C. elegans*. Firstly, we observed minor changes in synaptic vesicle (SV) morphology at synaptic regions in *fcho-1* mutants, suggesting that FCHO-1 may not play as critical a role at these specific sites of neuronal synapses compared to other endocytic proteins, such as endophilin (*unc-57*). Secondly, we found that the loss of FCHO-1 activity led to notable breaks in neuronal membranes, which correlated with an elevated exchange of cytoplasmic content between distinct neuronal cell types. This finding was particularly prominent in *fcho-1 null* mutants, indicating a distinct and essential role for FCHO-1 in preserving the integrity of neuronal boundaries. Lastly, we demonstrated that the sole expression of FCHO-1's APA domain was sufficient to restrict aberrant content exchange between neurons and maintain normal synaptic transmission. This implies that FCHO-1 operates through an AP-2 mediated pathway that is essential for maintaining neuronal boundaries and thereby ensuring proper neuronal function.

Several distinct modes of endocytosis support neuronal integrity

Given that endocytosis is central to safeguarding neuronal integrity, we will discuss FCHO-1 in the context of some of these endocytic processes.

Endocytosis of synaptic vesicles: The endocytosis of synaptic vesicles (SVs) can be achieved through kinetically distinguishable endocytic pathways that harbor a plethora of both distinct and shared proteins. FCHO-1 is commonly associated with clathrin-mediated endocytosis (CME), and despite reservations that its relatively slow kinetics can support the demands of synaptic activity, it is widely considered the major route for

synaptic vesicle (SV) endocytosis [28, 33, 34, 36-38, 42, 125]. As SV endocytosis is crucial for neuronal function, we first investigated whether the absence of FCHO-1 endocytic activity leads to indicative hallmarks of faulty SV retrieval. Our electron microscopy data illustrated that synaptic vesicle morphology at neuromuscular junctions (NMJs) are only moderately impaired (Figure 3, Figure 4). Additionally, the number of SVs at NMJs were similar to wild-type animals and *in vivo* VGLUT-pHluorin fluorescence recovery rates were not slowed in *fcho-1* mutants. In stark contrast, in *unc-57* mutant electron micrographs, we observed a severe depletion of SVs at NMJs, along with an *in vivo* accumulation of VGLUT-pHluorin fluorescence; both indicating a failure of protein retrieval from the membrane at endophilin mutant synapses. Though we do [88, 125] not believe that FCHO-1 is dispensable at these sites, this suggests that unlike UNC-57, FCHO-1 activity can be compensated for and less important at sites of SV retrieval in *C.elegans*. Albeit, the loss of individual AP-2 subunits does negatively impact SVs, suggesting that AP-2 cannot be compensated for synapses, irrespective of FCHO-1 activity. Nevertheless, the additive loss of FCHO-1 did not substantially exacerbate these phenotypes, implicating they largely work in a common pathway. To follow, our observation of prevalent neuronal breaks was distinct in *fcho-1* mutants, revealing a non-expendable role for FCHO-1 in maintaining neuronal boundaries, where UNC-57 activity, conversely, does not appear to influence this process. Taken together, these findings notion distinct roles for FCHO-1 and UNC-57 that are required at different sub-cellular regions of neurons. Furthermore, these data highlight that in events they do function in parallel at the same sites, there is a clear hierarchy in their necessity and the capacity to be compensated for.

Endocytosis of adhesion molecules: Neurons express multiple families of cell adhesion molecules (CAMs) [19, 25, 141, 142] known to regulate neuronal growth, synapse formation, and function. Though CAMs contribute to the stability and architecture of neuronal circuits, the nature of CAMs are dynamic, constantly being recycled from plasma membranes to accommodate the ever-changing needs of the cells via CME [143, 144]. Given CME dependent turnover of CAMS and perpetuity of neuronal breaks occurring at electron dense regions in *fcho-1* mutants, we explored whether FCHO-1, activity is necessary for proper recycling of SYG-1, a neuronal enriched CAM. We demonstrated that SYG-1 accumulated at synapses in *fcho-1* mutants, suggesting FCHO-1 may be important for its removal from neuronal membranes which may preemptively contribute to neuronal breaks. We speculate that the accumulation of these proteins leads to unequal tension between neighboring cells, ultimately generating the mechanical force that compromises the membrane's continuity. These data make way for future studies, where we are continuing to explore additional CAMs targeted by FCHO-1 how they are differentially regulated.

AP-2 and FCHO-1: FCHO-1 has a well-characterized relationship to AP-2, however the majority of studies have focused on their collaborative activity in non-neuronal cells. Furthermore, since knocking out all of AP-2's subunits is lethal, it has been difficult to comprehensively characterize its role in neurons. The viability of FCHO-1 mutants offers the opportunity to understand and discern where their collaboration is absolutely critical and instances where it is not. For example, AP-2 targeted endocytosis and the CME pathway have been proposed to function in the axon initial segment (AIS), to help

facilitate separation of axonal and dendritic compartments, which are morphologically and functionally distinct regions within neurons. In *C.elegans* and in rat hippocampal neurons, the loss of AP-2 abrogates AIS integrity, alluding to whether or not the AIS is also vulnerable in *fcho-1* mutants or if FCHO-1 can be compensated for. Our findings in conjunction with follow-up studies prompts the opportunity to comb apart how FCHO-1's activity is recruited, distributed, and prioritized within neurons which may provide additional clues about how FCHO-1 and AP-2 dependent endocytic programs are initiated and regulated holistically.

Content exchange and clinical implications

Few studies have reported neuronal cell-cell fusion, also reported as neuronal syncytia [145-149], that was coupled to axonal injury or viral perturbation. However, the consequences of these events remain elusive. Though similar in nature, the neuronal breaks and seemingly connected neuronal entities we observed, are not the result of an externally sourced impact, but rather an innate incompetence that can be linked to a potential pathway for FCHO-1 and AP-2. Data acquired via our PAGEN system exhibited that there is a substantial increase in neuronal exchange observed in *fcho-1* mutants *in vivo*, which suggests that cytosolic exchange may occur as a result of neuronal breaks and the loss of restrictive boundaries. Interestingly, this aberrant exchange can be halted with the sole expression of FCHO-1's APA domain, which informs us that FCHO-1 activation of AP-2 is important in preventing cytosolic exchange. Another plausible model delineating increased cytosolic exchange involves a role for FCHO-1-dependent endocytosis in response to breaks in neuronal membranes. Our PAGEN system also detected TEV protease exchange between classes of neurons

and minor instances of neuronal breaks in wild-type animals (Figure 5B, 4B), suggesting that these events do occur naturally, albeit infrequently. However, the substantial increase in neuronal exchange observed in *fcho-1* mutants may result from an inability to promptly repair these regions. Given the post-mitotic nature of neurons, it is sensible to assume that mechanisms exist in response to these occurrences, and several reports propose repair mechanisms relying on endocytosis [150-152]. For instance, the docking and fusion of vesicles to the plasma membrane can promote resealing by patching up the tear or decreasing membrane tension. In either proposed model for FCHO-1, cytosolic exchange persists which ultimately draws attention to the importance of safeguarding the integrity of neuronal membranes. To follow, we can consider the efforts that respond when it is compromised and expound on the associated consequences when timely interventions are lacking. Intriguing questions that arise from this study include: What happens to the identity of these neurons and the circuits they form? Additionally, can neuronal breaks accelerate the spread of pathogenic proteins that contribute to disease onset?

SUPPLEMENTARY FIGURES

Figure S1 Jimenez et al.

(Related to Figure 1)

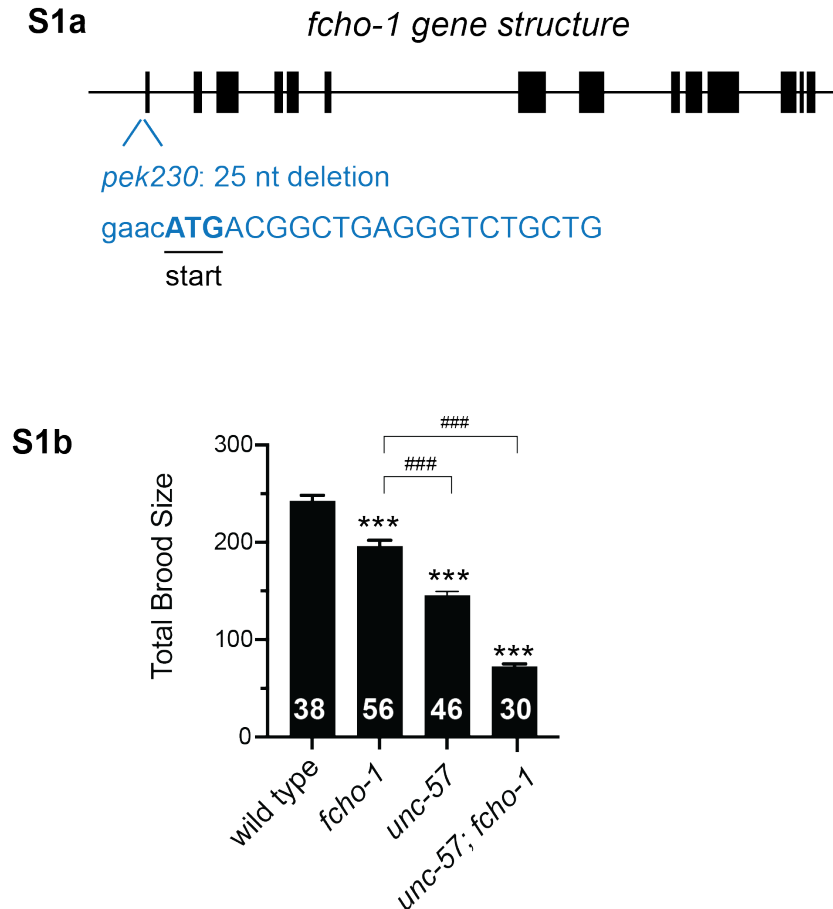


[Figure S1, related to Figure 1] Features of *fcho-1*(*pek230*) mutant

(A) There is a decrease in progeny of *fcho-1* mutants and an additive decrease in *fcho-1*; *unc-57* double mutants when compared to wild type animals. n number is individual animals and are indicated in bar graphs. ***, $p < 0.001$ when compared to wild type worms, and ###, $p < 0.001$ when compared to *fcho-1* mutants; one-way ANOVA followed by Dunnett's test. (B) A schematic demonstrating the gene structure of *fcho-1*. The *pek230* mutation derives from a 25 nucleotide (nt) deletion that includes the start codon.

Figure S2 Jimenez et al.

(Related to Figure 5)

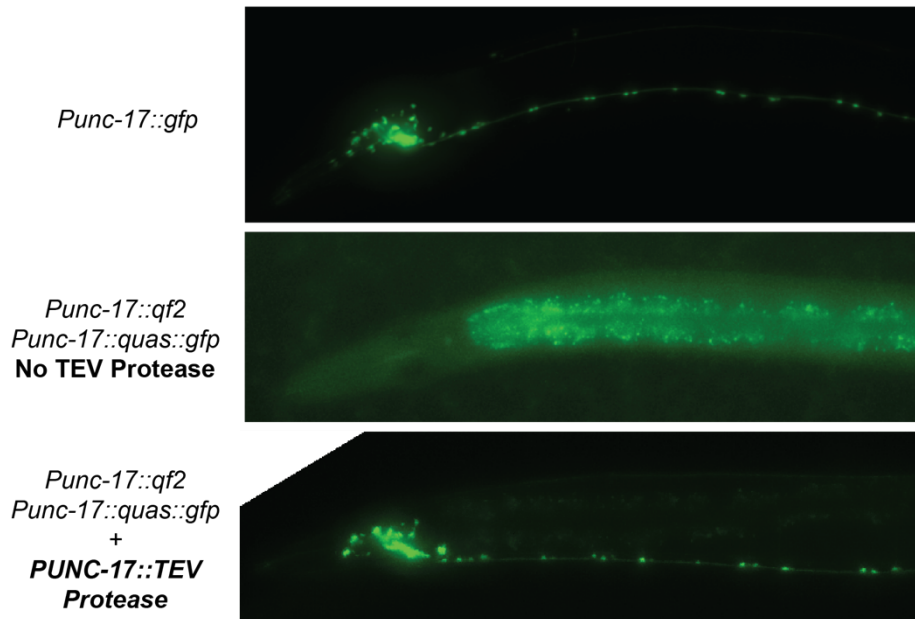


[Figure S2, related to Figure 5] PAGEN system can selectively activate GFP expression in cholinergic neurons using the *Punc-17* promoter

(Top panel) Single-copy insertion transgenes expressing cytosolic GFP under the *Punc-17* promoter in all cholinergic neurons (*Punc-17::gfp*). **(Middle panel)** PAGEN transgenic animals expressing anchored PUNC-17::QF2 and PUNC-17::QUAS::GFP. Since QF2 is anchored to the membrane, it is sequestered from the nucleus and cannot access the QUAS::gfp element thereby inhibiting GFP expression. **(Bottom Panel)** Same transgenic PAGEN animals as in middle panel, with the addition of PUNC-17::TEV protease. Expression of cholinergic TEV protease frees the cholinergic QF2 from the membrane and subsequently activating GFP expression in cholinergic neurons. Localization patterning of GFP expression in these PAGEN animals mimic

what is observed in single-copy transgenes (*Punc-17::gfp* ; *Top panel*), suggesting PAGEN induced GFP expression is confined to cholinergic neurons.

Figure S3 Jimenez et al.

(Related to Figure 6)

A.

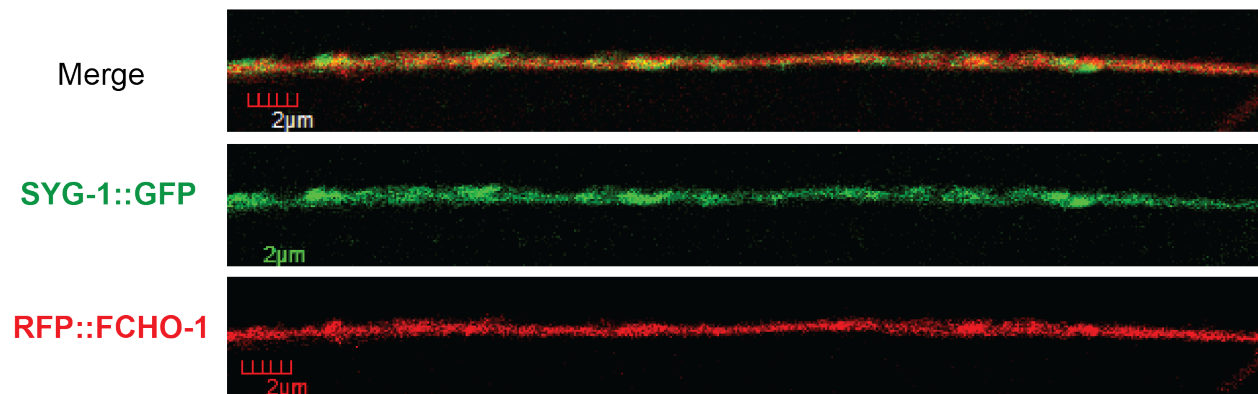


[Figure S3, related to Figure 6] SYG-1 and FCHO-1 are associated in synapses

(A) Representative images of SYG-1::GFP(A, middle) and RFP::FCHO-1(A, bottom) expressed in the dorsal cord. (A, Top) Merge is the overlay of both SYG-1::GFP and RFP::FCHO-1 demonstrating co-localization in dorsal DA neurons. Scale bar 2 µm.

Figure S4 Jimenez et al.

(Related to Figure 7)

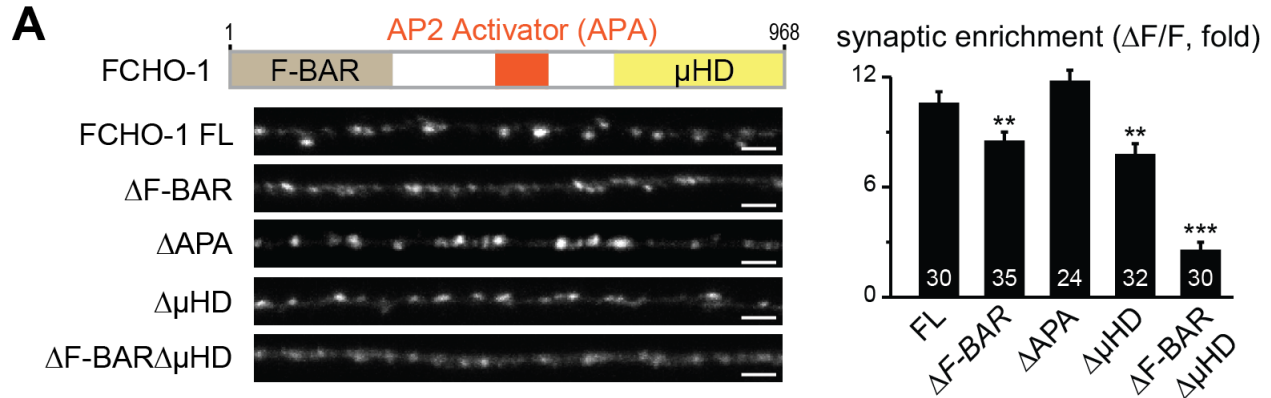


[Figure S4, related to Figure 7] The AP-2 Binding domain is likely not responsible for localization to synapses

(A, Left) Representative images of mutant RFP::FCHO-1 constructs in dorsal axons of DA neurons. Synaptic enrichment of indicated mutant genotype are quantified in **(A, Right)**. Synaptic enrichment RFP::FCHO-1 is decreased in of Δ F-BAR, Δ μ HD, and double mutant Δ F-BAR Δ μ HD mutant transgenes, indicating APA domain is not important for localization. Consistent, loss of APA domain does not impact enrichment levels at all, suggesting FCHO-1 enrichment in synapses is guided by the F-BAR and/or the μ HD. ** indicates $p < 0.001$, *** indicates $p < 0.0001$, compared to full length RFP::FCHO-1 (FL) controls. Student's t-test was used for statistical analyses. Error bars are standard error of the mean (SEM).

MATERIALS AND METHODS

Strains and DNA constructs

All *C.elegans* strains used for experimentation were maintained and genetically manipulated as previously described (Brenner et. al 1974). Strains were maintained at room temperature, 20°C, on agar nematode growth media (NGM) plates that were seeded with OP50 bacteria for animals to feed on. The N2 strain (Bristol, England) was used as the “wild-type” comparison to the *unc-57(e406)* transgene used in this study which was obtained from the Caenorhabditis Genetics Center and the *fcho-1 (pek230)* allele was derived from this study. DNA plasmids were constructed using the Multisite Gateway system (Invitrogen, Waltham, MA, USA) and Gibson assembly protocols [153]. All constructs were sequence verified. Additional strains used are provided in the table.

Transgenes and Germline Transformation

Transgenic strains were generated by microinjection. Mos1-mediated single-copy transgene insertion methods were used to produce animals carrying single-copy transgenes[154, 155]. Mos1 target sites used in this study are: ttTi5605 (II) to generate the *unc-57(e406)* and *fcho-1(pek230)* mutants and *cxTi10816* (chromosome IV) was used to generate the PAGEN lines (Quas::GFP + pekSi272[Punc-17::QF2-TEVsite-ALFA-TEVsite-unc-64FL::let-858utr+cb-unc-119(+)]cxTi10816IV). Transgenic worms were outcrossed at least 3 times.

Electrophysiology

Day-1 young adult hermaphrodite *C. elegans* were dissected, immobilized, and prepped as previously described [65, 124]. The prepped worm was mounted onto a fixed-stage upright microscope (BX51WI, Olympus) equipped with a 60x water-immersion objective

lens. The integrity of the anterior ventral body wall muscle and the ventral nerve cord were visually examined via the DIC microscopy, and ventral muscle cells were patched using fire-polished 2-5 M Ω resistant borosilicate pipettes (World Precision Instruments, USA). Whole-cell patch clamp recordings were carried out at 20°C. Body-wall muscle cells were voltage clamped at -60 mV to record postsynaptic currents. The currents were recorded in the whole-cell configuration from muscle cells using an amplifier (EPC-10; HEKA, Germany). Extracellular solution used as reported in Dong et al., 2015. Evoked EPSC responses were induced by applying a 0.4 ms, 30 μ A pulse, generated by a stimulus isolator (A365, WPI), through a borosilicate pipette (~2 M Ω) placed in close apposition to the ventral nerve cord. Series resistance was compensated to 70% for the evoked EPSC recording. All chemicals were purchased from Sigma. Data were sampled at 10 kHz using Patchmaster (HEKA), following low-pass filtering at 2 kHz. The number of animals for each experiment are provided in Figure legends.

Exploration assay

Exploration assays were performed on 6 cm nematode growth medium (NGM) plates uniformly seeded with the OP50 strain of *E. coli*. Individual young adults were placed in the center of each plate and left free to roam for 17 hours at room temperature (20°C). We placed the plates on top of transparency paper that was gridded with ~226 squares (each square 3mm x 3mm) and counted the number of squares that had remnant traces of the worms' travels. We analyzed ~20 animals for each mutant and repeated the experiments on three separate days. Average values and the standard error of the mean (SEM) were reported. P values were informed using an unpaired t test with Welch's correction.

Locomotion Assay

Young day 1 adult animals were picked onto 10 cm agar plates without a bacterial lawn (~30 worms per plate) and left to roam for an hour before imaging. Using WormLab Imaging System (MBF Bioscience, VT, USA), the crawling of individual worms was recorded for 30sec at 7.5fps. The center of mass was determined for each animal using custom object-tracking software developed using ImageJ (Schneider et al., 2012). The average speed distance traveled was determined for each animal. Reported averages are combined speeds from separate individual experimental runs.

VGLUT-pHluorin Imaging and Analysis

Worms carrying the *kyls673 [sra-6p::eat-4::pHluorin]* transgene were used for imaging VGLUT-pHluorin fluorescence as previously described[127]. Animals were loaded into custom-built PDMS microfluidic chambers designed to deliver stimuli under a fluorescent microscope[156]. To prevent movement, animals were paralyzed with 1mM tetramisole hydrochloride. NaCl stimulus (500mM) was prepared fresh daily in S. Basal Buffer. The ASH axons were imaged on an inverted Leica DMI8 microscope through a Leica PL APO 63x 1.40 NA oil immersion objective, onto an Andor iXon Life 888 EMCCD camera, using Leica LAS-X software. Animals were allowed to acclimate for 5 minutes in microfluidic chambers before imaging and were adapted to blue light for 90 seconds. No more than 3 trials were performed per animal. The time duration for all recording trials was 100 seconds, and the stimulus was presented for 10 seconds, starting at 30 seconds after imaging began and images were captured at 5 frames per second. Imaging analysis was performed as previously described[127]. Basal

fluorescence of VGLUT-pHluorin was obtained by averaging the first 10 seconds of each ROI for each trial after background correction. Decay curves were fitted and $\Delta F/F$ was determined as previously described. All imaging experiments for a given condition or observation were repeated on at least two separate days using independently prepared buffers and stimuli. The number of trials per animal and the total number of animals are reported along with the total trial number in the figure legends.

Transmission Electron Microscope for Visualizing Synaptic Vesicle

Approximately 10 adult hermaphrodites were quickly loaded into a 100 μm freezing chamber containing space-filling bacteria. These worms were frozen instantaneously at $\sim -180\text{ }^{\circ}\text{C}$ in a Leica EM PACT2 system. The frozen worms were fixed in a Leica EM AFS2 machine using 1% osmium in 0.1% UA in acetone fixative, then embedded in Eponate 12 from Ted Pella, Inc. Serial sections were cut at a thickness of 40 nm using an ultracut E microtome, collected on pioloform-covered slotted grids (notchnum 1x2 mm oval) from Ted Pella, Inc., and counterstained in 6% aqueous uranyl acetate for 1.5 hrs, followed by Reynolds lead citrate for 7 min. Images were obtained on a Talos L120C TEM transmission electron microscope (Thermo Fisher Scientific Inc, USA) operating at 120KV. Micrographs were collected using the Ceta-M 4k x 4k high-resolution camera (Thermo Fisher Scientific Inc, USA). Synapse profiles were used to count the number of synaptic vesicles at dense projections. Each profile represents a single section that passes through the dense projection. Measurements and quantification of synaptic vesicles were conducted using ImageJ measuring tools. P values were generated using one-way ANOVA followed by Dunnett's test.

PAGEN Assay

Single copy insertions of QUAS::GFP and cholinergic QF2 (*pekSi417[Punc-17::QF2-TEVsite-ALFA-TEVsite-unc-64FL::let-858_3'UTR + QUAS::GFP::unc-54utr + cb-unc-119(+)]cxTi10816 IVJ*) were generated using MosSCI techniques(see above), and subsequently microinjections were performed on these transgenes to express 15ng of dopaminergic TEV protease was expressed as extrachromosomal arrays (*PekEx2727[Punc-47::NbALFA::TEV protease::rab-3UTR; Pvha-6::mRuby]*). These transgenics were used as the controls (wild-type, wt) in these assays. These animals were subsequently crossed into *fcho-1* mutant animals and were selected for extrachromosomal co-injection marker (*Pvha-6::mRuby*) and *fcho-1* mutant jowls and genotyped to genotyped via PCR for MosSCI insertion and *fcho-1* mutant allele. All PAGEN transgenes used in this study were generated the same way and are provided in strains list. 30-40 young day 1 adults were randomly selected by array marker, paralyzed in 4uL of 50M Sodium azide (NaN₃), and imaged on an inverted Leica DMi8 microscope through a Leica PL APO 40X water immersion objective, onto an Andor iXon Life 888 EMCCD camera, using Leica LAS-X software. 488 nm laser scanner was used to ascertain and score number of animals expressing GFP. Statistical analyses performed and number of animals assayed are provided in figure legends.

Confocal Microscopy and Analysis

Worms were immobilized with 2,3-Butanedione monoxamine (30 mg/ml; Sigma-Aldrich), and were mounted on 2% agarose pads for imaging. Fluorescence images were collected on an inverted Olympus IX81 microscope, using a laser scanning confocal imaging system (Olympus FluoView FV1000) and an Olympus UPLSAPO 60x 1.4 NA

Oil immersion objective (at 5x zoom). GFP and mNeonGreen were excited using a 488 nm Argon laser and mScarlet was excited using a 559 nm diode pumped solid state laser. Dorsal nerve cords were imaged to determine synaptic and axonal distribution of all proteins examined in the study. Fluorescence images were analyzed using custom software in IGOR Pro (WaveMetrics, Lake Oswego, OR) [119, 157]. Images of fluorescent slides (Chroma Technology Group, VT) were collected daily to monitor the laser stability, and the dorsal cord fluorescence was normalized to the slide fluorescence value. Statistical significance was determined using one-way ANOVA or Student's t-test and all values reported are means \pm SEM.

Automated Image Analysis for SYG-1. Five image parameters were defined and collected using custom software scripts and IGOR Pro (WaveMetrics, Lake Oswego, OR) [119, 157] “Absolute peak fluorescence” (peak) is the ratio of peak fluorescence to the slide fluorescence value. “Absolute axon fluorescence” (axon) is the ratio of baseline fluorescence to the slide fluorescence value. “Baseline fluorescence” was identified as the minimum fluorescence level over a 5- μ m interval within the dorsal cord image. “Relative peak-to-axon magnitude” ($\% \Delta F/F$) is defined as $100 \cdot (F_{\text{peak}} - F_{\text{axon}})/F_{\text{axon}}$. “Width” is the distance between the points located halfway between peak and baseline on each side of the peak (full width at half maximum or FWHM). “Density” is the number of peaks found per 10 μ m of cord analyzed. N number is indicated in graph and figure legends.

Chapter 7:

Conclusions and Future Directions

Over the course of this thesis project, I have shed light on a role for FCHO-1 in the maintenance of cellular membrane integrity in neurons. Of note, this endocytic pathway is: 1) not dependent on endophilin/UNC-57 and (2) working in conjunction with the adaptor protein AP-2 and (3) suggestively regulates CAM protein SYG-1 enrichment on the plasma membrane (4) Results in an atypical exchange of cellular contents when this pathway is disrupted. In this discussion, I will expand on some of these findings and how they contribute to the current scientific field. I will discuss additional questions that have emerged from these findings and future experimental directions.

Models for FCHO-1 in neurons

A major question lingering from this study is whether these breaks are truly a consequence of lacking FCHO-1 activity or if FCHO-1 guiding a repair process that can no longer ensue. This question has been difficult to address since it is challenging to delineate what other proteins are involved. This undertaking is tricky because deletions of distinguishing endocytic proteins, such as AP-2, are lethal, or have a blanketed output of dysfunctions, thus making it hard isolate a tight link to additional proteins in this pathway. However, we speculate that it is the abundance of proteins, and eventual imbalance of tension, that generates the mechanical force that results in these breaks. We believe this to be true for three key reasons. Firstly, this exchange does not worsen with age (data not shown). If it was a repair mechanism was challenged, we would suspect an increase in neuronal disruption as neuronal integrity naturally occurs with age. It's also important to test whether neurons are merely dying and thus abrogating a

GFP signal altogether. Secondly, double *unc-54;fcho-1* mutants display an even greater exchange of neuronal content exchange. UNC-54 encodes a myosin chain protein that important for muscle movement. We hypothesized that a decrease in movement would correlate with a decrease in neuronal breaks and subsequent exchange, however we saw the opposite. This result sparks two follow up hypotheses: 1) that muscle integrity actually supports neuronal integrity and 2) suggests that neurons in *fcho-1* mutants are compromised, and can repair, from motor induced damage. And lastly, the identification of SYG-1 enrichment on neuronal PMs. This enrichment is a major indicator that the proteins governing neuronal connections specifically being are altered in *fcho-1* mutants.

Following up on these findings would include introducing AP-2 mutations that lock it into its “closed confirmation.” We hypothesize that in the *fcho-1* mutant, AP-2 is also accumulating on the PM along with SYG-1, and potentially other proteins, contributing to an unbalanced tension between neurons. Results from this experiment would reveal key components of this FCHO-1 pathway. Specifically, this experiment would help us discern if FCHO-1 is the regulatory component alluring AP-2 to these sites. If AP-2 is accumulating on the membrane, this would suggest that it is simply not being activated at these sites. On the contrary, we may find that AP-2 does not accumulate at these sites, suggesting that FCHO-1 is the primary initiator in these instances.

FCHO-1 and synaptic vesicle recycling

In the context of *C. elegans*, our data adds to the ongoing model that CME is not

primary route for SV retrieval at PM's in neurons. This is demonstrated by the stable pool of SVs found in *fcho-1* mutant synapses. Consistent with the field, the modest changes in the size of vesicles found at synaptic regions, may indicate that CME be necessary for subsequent synaptic vesicle (SV) regeneration from larger endosomes after their retrieval from the plasma membrane PM via bulk endocytosis. This observation becomes particularly insightful, as it strongly implies that the synaptic transmission defects observed in *fcho-1* mutants are largely not attributed to a mis-regulation or shortage within the synaptic vesicle pool. Future experiments investigating the consequences of the neuronal breaks, discussed here later, will help us better understand the source of diminished synaptic activity associated with *fcho-1* loss.

What other PM targets and what other pathways?

The CAM SYG-1 was an ideal candidate in due part to its neuronal enrichment, however, there are a whole host of CAMs found in neurons that could also be targeted by this FCHO-1 reliant pathway. Additionally, there are several families of adhesion molecules that stabilize neurons, including cadherins and integrins [158]. Identifying an exhaustive list of targets for FCHO-1 would ultimately help us discern how the regulatory component of these endocytic pathways. It may be possible that FCHO-1 only targets a sub-set of these proteins, which we can then delineate how and for what intended purpose. This then sets the stage for identifying additional non-FCHO-1 dependent routes that similarly can impact the structural integrity of neurons. To address this possibility, we can utilize the PAGEN assay as a tool to perform another genetic screen whereby we can identify mutants that have an even greater exchange of cytosolic exchange.

What are biological consequences of these breaks?

Our most notable observation from this study was the resulting prevalence of cytosolic content sharing. Two working hypotheses is that the morphological defects observed in *fcho-1* mutants alter the activity pattern in neural circuits and that these structural defects can allow toxic factors to spread and damage neighboring neurons. A neural circuit is composed of neurons with distinct properties. For example, cholinergic neurons send excitatory neurotransmitters, while GABAergic neurons release inhibitory signals. Importantly, functional outputs from any circuit are results of precisely patterned activities of individual neurons in the network. Alterations of neuronal connectivity are expected to disrupt the flow of information, and thereafter change the circuit outputs. To address the possibility that the identity of neurons can be altered, in future experiments we can stimulate neurons using an optogenetic approach and track the Ca^{2+} signals in stimulated neurons, as well as their neighboring neurons, using the Ca^{2+} reporter GCaMP6. In event that the spreading of Ca^{2+} among neighboring neurons occurs, then I would observe that the activities of different classes of neurons are abnormally coupled. To measure neuronal outputs, we can record excitatory and inhibitory postsynaptic currents at neuromuscular junctions. Results from these studies will define the role of FCHO-1 in maintaining circuit function by protecting neurons from interferences by neighbors. The exchange of Ca^{2+} is an ideal starting point to link the negative impact lacking FCHO-1 has on synaptic transmission.

On the other side of this coin, it's curious to consider what this cytosolic exchange means in the context of neurological disorders. As mentioned in Chapter 3, several neurological diseases have been linked to CME dysfunction, thus prompting the

question of FCHO-1 involvement. Additionally, the breaks that arise in *fcho-1* mutants now begs the question whether this provides an avenue for an expedited exchange of toxic aggregates between neighboring neurons. It is well established that protein aggregation is a major factor that facilitates the progression of neurodegeneration. In humans, at least nine neurodegenerative diseases are linked to the expansion of glutamine repeats (polyQ). These polyQ repeats are prone to the formation of misfolded aggregates, which are thought to induce neuron death [159, 160]. In future studies, I hope to explore a potential connection between FCHO-1 and mutant huntingtin (mHTT). Several studies found that the polyQ protein mHTT undergoes transcellular spreading, which may enhance the deleterious effects during the propagation of Huntington's Disease [161, 162]. However, the requirement of rapid spreading among neurons is consistent in the several neurological disorders, including Alzheimer's Disease. Exploration of this hypothesis can help us address key questions including, does mHTT impair the contact sites of neurons? Are more mHTT aggregates spread to neighboring neurons in *fcho-1* mutants? Does FCHO-1 removal lead to early onset of behavioral defects in mHTT worms? Together, these studies may uncover an important role of FCHO-1 in the progression of pathological aggregates. Largely, the *fcho-1* mutant can serve as tool to study a number of disease models, that can mutually support our learning of endocytic models in neurons and the progression and onset of a myriad of neuronal disorders.

Bibliography

1. Parton, R.G. and C.G. Dotti, *Cell biology of neuronal endocytosis*. J Neurosci Res, 1993. **36**(1): p. 1-9.
2. Kaksonen, M. and A. Roux, *Mechanisms of clathrin-mediated endocytosis*. Nat Rev Mol Cell Biol, 2018. **19**(5): p. 313-326.
3. McMahon, H.T. and E. Boucrot, *Molecular mechanism and physiological functions of clathrin-mediated endocytosis*. Nat Rev Mol Cell Biol, 2011. **12**(8): p. 517-33.
4. Lim, J.P. and P.A. Gleeson, *Macropinocytosis: an endocytic pathway for internalising large gulps*. Immunol Cell Biol, 2011. **89**(8): p. 836-43.
5. Bentley, M. and G. Banker, *The cellular mechanisms that maintain neuronal polarity*. Nat Rev Neurosci, 2016. **17**(10): p. 611-22.
6. Sampo, B., S. Kaech, S. Kunz, and G. Banker, *Two distinct mechanisms target membrane proteins to the axonal surface*. Neuron, 2003. **37**(4): p. 611-24.
7. Garrido, J.J., et al., *Identification of an axonal determinant in the C-terminus of the sodium channel Na(v)1.2*. EMBO J, 2001. **20**(21): p. 5950-61.
8. Guo, X., G.G. Farias, R. Mattera, and J.S. Bonifacino, *Rab5 and its effector FHF contribute to neuronal polarity through dynein-dependent retrieval of somatodendritic proteins from the axon*. Proc Natl Acad Sci U S A, 2016. **113**(36): p. E5318-27.
9. Palay, S.L., C. Sotelo, A. Peters, and P.M. Orkand, *The axon hillock and the initial segment*. J Cell Biol, 1968. **38**(1): p. 193-201.
10. Huang, C.Y. and M.N. Rasband, *Axon initial segments: structure, function, and disease*. Ann N Y Acad Sci, 2018. **1420**(1): p. 46-61.
11. Eichel, K., et al., *Endocytosis in the axon initial segment maintains neuronal polarity*. Nature, 2022. **609**(7925): p. 128-135.
12. Nelson, A.D. and P.M. Jenkins, *Axonal Membranes and Their Domains: Assembly and Function of the Axon Initial Segment and Node of Ranvier*. Front Cell Neurosci, 2017. **11**: p. 136.
13. Garrido, J.J., et al., *A targeting motif involved in sodium channel clustering at the axonal initial segment*. Science, 2003. **300**(5628): p. 2091-4.
14. Torii, T., et al., *NuMA1 promotes axon initial segment assembly through inhibition of endocytosis*. J Cell Biol, 2020. **219**(2).
15. Yap, C.C. and B. Winckler, *Harnessing the power of the endosome to regulate neural development*. Neuron, 2012. **74**(3): p. 440-51.
16. Yap, C.C. and B. Winckler, *Adapting for endocytosis: roles for endocytic sorting adaptors in directing neural development*. Front Cell Neurosci, 2015. **9**: p. 119.

17. Ezratty, E.J., C. Bertaux, E.E. Marcantonio, and G.G. Gundersen, *Clathrin mediates integrin endocytosis for focal adhesion disassembly in migrating cells*. J Cell Biol, 2009. **187**(5): p. 733-47.
18. Chao, W.T. and J. Kunz, *Focal adhesion disassembly requires clathrin-dependent endocytosis of integrins*. FEBS Lett, 2009. **583**(8): p. 1337-43.
19. Kawauchi, T., *Cell adhesion and its endocytic regulation in cell migration during neural development and cancer metastasis*. Int J Mol Sci, 2012. **13**(4): p. 4564-4590.
20. Wilkinson, R.S. and M.Y. Lin, *Endocytosis and synaptic plasticity: might the tail wag the dog?* Trends Neurosci, 2004. **27**(4): p. 171-4.
21. Heckman, E.L. and C.Q. Doe, *Establishment and Maintenance of Neural Circuit Architecture*. J Neurosci, 2021. **41**(6): p. 1119-1129.
22. Juliano, R.L., *Signal transduction by cell adhesion receptors and the cytoskeleton: functions of integrins, cadherins, selectins, and immunoglobulin-superfamily members*. Annu Rev Pharmacol Toxicol, 2002. **42**: p. 283-323.
23. Maness, P.F. and M. Schachner, *Neural recognition molecules of the immunoglobulin superfamily: signaling transducers of axon guidance and neuronal migration*. Nat Neurosci, 2007. **10**(1): p. 19-26.
24. Leshchyns'ka, I. and V. Sytnyk, *Reciprocal Interactions between Cell Adhesion Molecules of the Immunoglobulin Superfamily and the Cytoskeleton in Neurons*. Front Cell Dev Biol, 2016. **4**: p. 9.
25. Kozlova, I., et al., *Cell Adhesion Molecules and Protein Synthesis Regulation in Neurons*. Front Mol Neurosci, 2020. **13**: p. 592126.
26. Sudhof, T.C., *The synaptic vesicle cycle*. Annu Rev Neurosci, 2004. **27**: p. 509-47.
27. Wu, L.G., E. Hamid, W. Shin, and H.C. Chiang, *Exocytosis and endocytosis: modes, functions, and coupling mechanisms*. Annu Rev Physiol, 2014. **76**: p. 301-31.
28. Gan, Q. and S. Watanabe, *Synaptic Vesicle Endocytosis in Different Model Systems*. Front Cell Neurosci, 2018. **12**: p. 171.
29. Milosevic, I., *Spatial and Temporal Aspects of Phosphoinositides in Endocytosis Studied in the Isolated Plasma Membranes*. Methods Mol Biol, 2018. **1847**: p. 147-160.
30. Kirchhausen, T., *Clathrin*. Annu Rev Biochem, 2000. **69**: p. 699-727.
31. Kirchhausen, T., *Imaging endocytic clathrin structures in living cells*. Trends Cell Biol, 2009. **19**(11): p. 596-605.
32. Edeling, M.A., C. Smith, and D. Owen, *Life of a clathrin coat: insights from clathrin and AP structures*. Nat Rev Mol Cell Biol, 2006. **7**(1): p. 32-44.
33. Dittman, J. and T.A. Ryan, *Molecular circuitry of endocytosis at nerve terminals*. Annu Rev Cell Dev Biol, 2009. **25**: p. 133-60.

34. Granseth, B., B. Odermatt, S.J. Royle, and L. Lagnado, *Clathrin-mediated endocytosis is the dominant mechanism of vesicle retrieval at hippocampal synapses*. *Neuron*, 2006. **51**(6): p. 773-86.
35. Kim, S.H. and T.A. Ryan, *Synaptic vesicle recycling at CNS synapses without AP-2*. *J Neurosci*, 2009. **29**(12): p. 3865-74.
36. Saheki, Y. and P. De Camilli, *Synaptic vesicle endocytosis*. *Cold Spring Harb Perspect Biol*, 2012. **4**(9): p. a005645.
37. Blondeau, F., et al., *Tandem MS analysis of brain clathrin-coated vesicles reveals their critical involvement in synaptic vesicle recycling*. *Proc Natl Acad Sci U S A*, 2004. **101**(11): p. 3833-8.
38. Maycox, P.R., et al., *Clathrin-coated vesicles in nervous tissue are involved primarily in synaptic vesicle recycling*. *J Cell Biol*, 1992. **118**(6): p. 1379-88.
39. Kononenko, N.L., et al., *Compromised fidelity of endocytic synaptic vesicle protein sorting in the absence of stonin 2*. *Proc Natl Acad Sci U S A*, 2013. **110**(6): p. E526-35.
40. Koo, S.J., et al., *Vesicular Synaptobrevin/VAMP2 Levels Guarded by AP180 Control Efficient Neurotransmission*. *Neuron*, 2015. **88**(2): p. 330-44.
41. Voglmaier, S.M., et al., *Distinct endocytic pathways control the rate and extent of synaptic vesicle protein recycling*. *Neuron*, 2006. **51**(1): p. 71-84.
42. Diril, M.K., et al., *Stonin 2 is an AP-2-dependent endocytic sorting adaptor for synaptotagmin internalization and recycling*. *Dev Cell*, 2006. **10**(2): p. 233-44.
43. Jung, N. and V. Haucke, *Clathrin-mediated endocytosis at synapses*. *Traffic*, 2007. **8**(9): p. 1129-36.
44. Maritzen, T., S.J. Koo, and V. Haucke, *Turning CALM into excitement: AP180 and CALM in endocytosis and disease*. *Biol Cell*, 2012. **104**(10): p. 588-602.
45. Kaempfer, N., et al., *Overlapping functions of stonin 2 and SV2 in sorting of the calcium sensor synaptotagmin 1 to synaptic vesicles*. *Proc Natl Acad Sci U S A*, 2015. **112**(23): p. 7297-302.
46. Heerssen, H., R.D. Fetter, and G.W. Davis, *Clathrin dependence of synaptic-vesicle formation at the *Drosophila* neuromuscular junction*. *Curr Biol*, 2008. **18**(6): p. 401-9.
47. Kononenko, N.L., et al., *Clathrin/AP-2 mediate synaptic vesicle reformation from endosome-like vacuoles but are not essential for membrane retrieval at central synapses*. *Neuron*, 2014. **82**(5): p. 981-8.
48. Watanabe, S., et al., *Clathrin regenerates synaptic vesicles from endosomes*. *Nature*, 2014. **515**(7526): p. 228-33.
49. Milosevic, I., et al., *Recruitment of endophilin to clathrin-coated pit necks is required for efficient vesicle uncoating after fission*. *Neuron*, 2011. **72**(4): p. 587-601.

50. Ferguson, S.M., et al., *Coordinated actions of actin and BAR proteins upstream of dynamin at endocytic clathrin-coated pits*. *Dev Cell*, 2009. **17**(6): p. 811-22.
51. Di Paolo, G., et al., *Recruitment and regulation of phosphatidylinositol phosphate kinase type 1 gamma by the FERM domain of talin*. *Nature*, 2002. **420**(6911): p. 85-9.
52. Ceccarelli, B., W.P. Hurlbut, and A. Mauro, *Turnover of transmitter and synaptic vesicles at the frog neuromuscular junction*. *J Cell Biol*, 1973. **57**(2): p. 499-524.
53. Nonet, M.L., et al., *UNC-11, a Caenorhabditis elegans AP180 homologue, regulates the size and protein composition of synaptic vesicles*. *Mol Biol Cell*, 1999. **10**(7): p. 2343-60.
54. Gandhi, S.P. and C.F. Stevens, *Three modes of synaptic vesicular recycling revealed by single-vesicle imaging*. *Nature*, 2003. **423**(6940): p. 607-13.
55. Zhang, S., et al., *Size-Dependent Endocytosis of Nanoparticles*. *Adv Mater*, 2009. **21**: p. 419-424.
56. Heuser, J.E. and T.S. Reese, *Evidence for recycling of synaptic vesicle membrane during transmitter release at the frog neuromuscular junction*. *J Cell Biol*, 1973. **57**(2): p. 315-44.
57. Miller, T.M. and J.E. Heuser, *Endocytosis of synaptic vesicle membrane at the frog neuromuscular junction*. *J Cell Biol*, 1984. **98**(2): p. 685-98.
58. Holt, M., A. Cooke, M.M. Wu, and L. Lagnado, *Bulk membrane retrieval in the synaptic terminal of retinal bipolar cells*. *J Neurosci*, 2003. **23**(4): p. 1329-39.
59. Paillart, C., J. Li, G. Matthews, and P. Sterling, *Endocytosis and vesicle recycling at a ribbon synapse*. *J Neurosci*, 2003. **23**(10): p. 4092-9.
60. Watanabe, S. and E. Boucrot, *Fast and ultrafast endocytosis*. *Curr Opin Cell Biol*, 2017. **47**: p. 64-71.
61. Watanabe, S., et al., *Ultrafast endocytosis at Caenorhabditis elegans neuromuscular junctions*. *Elife*, 2013. **2**: p. e00723.
62. Verstreken, P., et al., *Synaptojanin is recruited by endophilin to promote synaptic vesicle uncoating*. *Neuron*, 2003. **40**(4): p. 733-48.
63. Watanabe, S., et al., *Synaptojanin and Endophilin Mediate Neck Formation during Ultrafast Endocytosis*. *Neuron*, 2018. **98**(6): p. 1184-1197 e6.
64. Bai, J., et al., *Endophilin functions as a membrane-bending molecule and is delivered to endocytic zones by exocytosis*. *Cell*, 2010. **143**(3): p. 430-41.
65. Richmond, J.E. and E.M. Jorgensen, *One GABA and two acetylcholine receptors function at the C. elegans neuromuscular junction*. *Nat Neurosci*, 1999. **2**(9): p. 791-7.
66. Jorgensen, E.M., et al., *Defective recycling of synaptic vesicles in synaptotagmin mutants of Caenorhabditis elegans*. *Nature*, 1995. **378**(6553): p. 196-9.

67. Mullen, G.P., et al., *UNC-41/stonin functions with AP2 to recycle synaptic vesicles in Caenorhabditis elegans*. PLoS One, 2012. **7**(7): p. e40095.
68. Kittelmann, M., et al., *In vivo synaptic recovery following optogenetic hyperstimulation*. Proc Natl Acad Sci U S A, 2013. **110**(32): p. E3007-16.
69. Watanabe, S., et al., *Ultrafast endocytosis at mouse hippocampal synapses*. Nature, 2013. **504**(7479): p. 242-247.
70. Soykan, T., et al., *Synaptic Vesicle Endocytosis Occurs on Multiple Timescales and Is Mediated by Formin-Dependent Actin Assembly*. Neuron, 2017. **93**(4): p. 854-866 e4.
71. Kaksonen, M., C.P. Toret, and D.G. Drubin, *A modular design for the clathrin- and actin-mediated endocytosis machinery*. Cell, 2005. **123**(2): p. 305-20.
72. Merrifield, C.J., M.E. Feldman, L. Wan, and W. Almers, *Imaging actin and dynamin recruitment during invagination of single clathrin-coated pits*. Nat Cell Biol, 2002. **4**(9): p. 691-8.
73. Taylor, M.J., D. Perrais, and C.J. Merrifield, *A high precision survey of the molecular dynamics of mammalian clathrin-mediated endocytosis*. PLoS Biol, 2011. **9**(3): p. e1000604.
74. Tonikian, R., et al., *Bayesian modeling of the yeast SH3 domain interactome predicts spatiotemporal dynamics of endocytosis proteins*. PLoS Biol, 2009. **7**(10): p. e1000218.
75. Maldonado-Baez, L. and B. Wendland, *Endocytic adaptors: recruiters, coordinators and regulators*. Trends Cell Biol, 2006. **16**(10): p. 505-13.
76. Keen, J.H., *Clathrin assembly proteins: affinity purification and a model for coat assembly*. J Cell Biol, 1987. **105**(5): p. 1989-98.
77. Simpson, F., A.A. Peden, L. Christopoulou, and M.S. Robinson, *Characterization of the adaptor-related protein complex, AP-3*. J Cell Biol, 1997. **137**(4): p. 835-45.
78. Dell'Angelica, E.C., C. Mullins, and J.S. Bonifacino, *AP-4, a novel protein complex related to clathrin adaptors*. J Biol Chem, 1999. **274**(11): p. 7278-85.
79. Hirst, J., et al., *The fifth adaptor protein complex*. PLoS Biol, 2011. **9**(10): p. e1001170.
80. Lee, J., G.D. Jongeward, and P.W. Sternberg, *unc-101, a gene required for many aspects of Caenorhabditis elegans development and behavior, encodes a clathrin-associated protein*. Genes Dev, 1994. **8**(1): p. 60-73.
81. Shim, J. and J. Lee, *The AP-3 clathrin-associated complex is essential for embryonic and larval development in Caenorhabditis elegans*. Mol Cells, 2005. **19**(3): p. 452-7.
82. Shim, J., P.W. Sternberg, and J. Lee, *Distinct and redundant functions of mu1 medium chains of the AP-1 clathrin-associated protein complex in the nematode Caenorhabditis elegans*. Mol Biol Cell, 2000. **11**(8): p. 2743-56.

83. Grant, B. and D. Hirsh, *Receptor-mediated endocytosis in the Caenorhabditis elegans oocyte*. Mol Biol Cell, 1999. **10**(12): p. 4311-26.
84. Owen, D.J., B.M. Collins, and P.R. Evans, *Adaptors for clathrin coats: structure and function*. Annu Rev Cell Dev Biol, 2004. **20**: p. 153-91.
85. Robinson, M.S., *Adaptable adaptors for coated vesicles*. Trends Cell Biol, 2004. **14**(4): p. 167-74.
86. Schmid, E.M. and H.T. McMahon, *Integrating molecular and network biology to decode endocytosis*. Nature, 2007. **448**(7156): p. 883-8.
87. Traub, L.M., *Tickets to ride: selecting cargo for clathrin-regulated internalization*. Nat Rev Mol Cell Biol, 2009. **10**(9): p. 583-96.
88. Hollopeter, G., et al., *The membrane-associated proteins FCHo and SGIP are allosteric activators of the AP2 clathrin adaptor complex*. Elife, 2014. **3**.
89. Ma, L., et al., *Transient Fcho1/2·Eps15/R·AP-2 Nanoclusters Prime the AP-2 Clathrin Adaptor for Cargo Binding*. Dev Cell, 2016. **37**(5): p. 428-43.
90. Umasankar, P.K., et al., *A clathrin coat assembly role for the muniscin protein central linker revealed by TALEN-mediated gene editing*. Elife, 2014. **3**.
91. Beacham, G.M., E.A. Partlow, J.J. Lange, and G. Hollopeter, *NECAPs are negative regulators of the AP2 clathrin adaptor complex*. Elife, 2018. **7**.
92. Gonzalez-Gaitan, M. and H. Jackle, *Role of Drosophila alpha-adaptin in presynaptic vesicle recycling*. Cell, 1997. **88**(6): p. 767-76.
93. Mitsunari, T., et al., *Clathrin adaptor AP-2 is essential for early embryonal development*. Mol Cell Biol, 2005. **25**(21): p. 9318-23.
94. Reider, A., et al., *Syp1 is a conserved endocytic adaptor that contains domains involved in cargo selection and membrane tubulation*. EMBO J, 2009. **28**(20): p. 3103-16.
95. Uezu, A., et al., *Characterization of the EFC/F-BAR domain protein, FCHO2*. Genes Cells, 2011. **16**(8): p. 868-78.
96. Zaccai, N.R., et al., *FCHO controls AP2's initiating role in endocytosis through a PtdIns(4,5)P(2)-dependent switch*. Sci Adv, 2022. **8**(17): p. eabn2018.
97. Henne, W.M., et al., *FCHo proteins are nucleators of clathrin-mediated endocytosis*. Science, 2010. **328**(5983): p. 1281-4.
98. Henne, W.M., et al., *Structure and analysis of FCHo2 F-BAR domain: a dimerizing and membrane recruitment module that effects membrane curvature*. Structure, 2007. **15**(7): p. 839-52.
99. Stimpson, H.E., et al., *Early-arriving Syp1p and Ede1p function in endocytic site placement and formation in budding yeast*. Mol Biol Cell, 2009. **20**(22): p. 4640-51.

100. Calzoni, E., et al., *F-BAR domain only protein 1 (FCHO1) deficiency is a novel cause of combined immune deficiency in human subjects*. J Allergy Clin Immunol, 2019. **143**(6): p. 2317-2321 e12.
101. Lyszkiewicz, M., et al., *Human FCHO1 deficiency reveals role for clathrin-mediated endocytosis in development and function of T cells*. Nat Commun, 2020. **11**(1): p. 1031.
102. Cocucci, E., F. Aguet, S. Boulant, and T. Kirchhausen, *The first five seconds in the life of a clathrin-coated pit*. Cell, 2012. **150**(3): p. 495-507.
103. Umasankar, P.K., et al., *Distinct and separable activities of the endocytic clathrin-coat components Fcho1/2 and AP-2 in developmental patterning*. Nat Cell Biol, 2012. **14**(5): p. 488-501.
104. Ritter, B., et al., *NECAP 1 regulates AP-2 interactions to control vesicle size, number, and cargo during clathrin-mediated endocytosis*. PLoS Biol, 2013. **11**(10): p. e1001670.
105. Dhindsa, R.S., et al., *Epileptic encephalopathy-causing mutations in DNMI1 impair synaptic vesicle endocytosis*. Neurol Genet, 2015. **1**(1): p. e4.
106. Helbig, I., et al., *A Recurrent Missense Variant in AP2M1 Impairs Clathrin-Mediated Endocytosis and Causes Developmental and Epileptic Encephalopathy*. Am J Hum Genet, 2019. **104**(6): p. 1060-1072.
107. Schubert, K.O., M. Focking, J.H. Prehn, and D.R. Cotter, *Hypothesis review: are clathrin-mediated endocytosis and clathrin-dependent membrane and protein trafficking core pathophysiological processes in schizophrenia and bipolar disorder?* Mol Psychiatry, 2012. **17**(7): p. 669-81.
108. McAdam, R.L., et al., *Loss of huntingtin function slows synaptic vesicle endocytosis in striatal neurons from the htt(Q140/Q140) mouse model of Huntington's disease*. Neurobiol Dis, 2020. **134**: p. 104637.
109. Vidyadhara, D.J., J.E. Lee, and S.S. Chandra, *Role of the endolysosomal system in Parkinson's disease*. J Neurochem, 2019. **150**(5): p. 487-506.
110. Imai, Y., et al., *The Parkinson's Disease-Associated Protein Kinase LRRK2 Modulates Notch Signaling through the Endosomal Pathway*. PLoS Genet, 2015. **11**(9): p. e1005503.
111. Ando, K., et al., *Alzheimer's Disease: Tau Pathology and Dysfunction of Endocytosis*. Front Mol Neurosci, 2020. **13**: p. 583755.
112. Palmer, A.M., *Neuroprotective therapeutics for Alzheimer's disease: progress and prospects*. Trends Pharmacol Sci, 2011. **32**(3): p. 141-7.
113. Wu, F. and P.J. Yao, *Clathrin-mediated endocytosis and Alzheimer's disease: an update*. Ageing Res Rev, 2009. **8**(3): p. 147-9.
114. Murdoch, J.D., et al., *Endophilin-A Deficiency Induces the Foxo3a-Fbxo32 Network in the Brain and Causes Dysregulation of Autophagy and the Ubiquitin-Proteasome System*. Cell Rep, 2016. **17**(4): p. 1071-1086.

115. Cao, M., et al., *Parkinson Sac Domain Mutation in Synaptojanin 1 Impairs Clathrin Uncoating at Synapses and Triggers Dystrophic Changes in Dopaminergic Axons*. *Neuron*, 2017. **93**(4): p. 882-896 e5.
116. Krebs, C.E., et al., *The Sac1 domain of SYNJ1 identified mutated in a family with early-onset progressive Parkinsonism with generalized seizures*. *Hum Mutat*, 2013. **34**(9): p. 1200-7.
117. Yao, P.J. and P.D. Coleman, *Reduced O-glycosylated clathrin assembly protein AP180: implication for synaptic vesicle recycling dysfunction in Alzheimer's disease*. *Neurosci Lett*, 1998. **252**(1): p. 33-6.
118. Schreij, A.M., E.A. Fon, and P.S. McPherson, *Endocytic membrane trafficking and neurodegenerative disease*. *Cell Mol Life Sci*, 2016. **73**(8): p. 1529-45.
119. Dittman, J.S. and J.M. Kaplan, *Factors regulating the abundance and localization of synaptobrevin in the plasma membrane*. *Proc Natl Acad Sci U S A*, 2006. **103**(30): p. 11399-404.
120. Katoh, M. and M. Katoh, *Identification and characterization of human FCHO2 and mouse Fcho2 genes in silico*. *Int J Mol Med*, 2004. **14**(2): p. 327-31.
121. Lee, S.E., et al., *SGIP1alpha, but Not SGIP1, is an Ortholog of FCHO Proteins and Functions as an Endocytic Regulator*. *Front Cell Dev Biol*, 2021. **9**: p. 801420.
122. Boucrot, E., et al., *Endophilin marks and controls a clathrin-independent endocytic pathway*. *Nature*, 2015. **517**(7535): p. 460-5.
123. Renard, H.F., et al., *Endophilin-A2 functions in membrane scission in clathrin-independent endocytosis*. *Nature*, 2015. **517**(7535): p. 493-6.
124. Dong, Y., et al., *Synaptojanin cooperates in vivo with endophilin through an unexpected mechanism*. *Elife*, 2015. **4**.
125. Gu, M., et al., *AP2 hemicomplexes contribute independently to synaptic vesicle endocytosis*. *Elife*, 2013. **2**: p. e00190.
126. Gu, M., et al., *Mu2 adaptin facilitates but is not essential for synaptic vesicle recycling in Caenorhabditis elegans*. *J Cell Biol*, 2008. **183**(5): p. 881-92.
127. Ventimiglia, D. and C.I. Bargmann, *Diverse modes of synaptic signaling, regulation, and plasticity distinguish two classes of C. elegans glutamatergic neurons*. *Elife*, 2017. **6**.
128. Zhang, L., et al., *The endophilin curvature-sensitive motif requires electrostatic guidance to recycle synaptic vesicles in vivo*. *Dev Cell*, 2022. **57**(6): p. 750-766 e5.
129. Wei, X., C.J. Potter, L. Luo, and K. Shen, *Controlling gene expression with the Q repressible binary expression system in Caenorhabditis elegans*. *Nat Methods*, 2012. **9**(4): p. 391-5.

130. Tucker, D.K., C.S. Adams, G. Prasad, and B.D. Ackley, *The Immunoglobulin Superfamily Members syg-2 and syg-1 Regulate Neurite Development in C. elegans*. *J Dev Biol*, 2022. **10**(1).
131. Chao, D.L. and K. Shen, *Functional dissection of SYG-1 and SYG-2, cell adhesion molecules required for selective synaptogenesis in C. elegans*. *Mol Cell Neurosci*, 2008. **39**(2): p. 248-57.
132. Ozkan, E., et al., *Extracellular architecture of the SYG-1/SYG-2 adhesion complex instructs synaptogenesis*. *Cell*, 2014. **156**(3): p. 482-94.
133. Chia, P.H., et al., *Local F-actin network links synapse formation and axon branching*. *Cell*, 2014. **156**(1-2): p. 208-20.
134. Shen, K. and C.I. Bargmann, *The immunoglobulin superfamily protein SYG-1 determines the location of specific synapses in C. elegans*. *Cell*, 2003. **112**(5): p. 619-30.
135. Colavita, A., et al., *Pioneer axon guidance by UNC-129, a C. elegans TGF-beta*. *Science*, 1998. **281**(5377): p. 706-9.
136. Verstreken, P., et al., *Endophilin mutations block clathrin-mediated endocytosis but not neurotransmitter release*. *Cell*, 2002. **109**(1): p. 101-12.
137. Schuske, K.R., et al., *Endophilin is required for synaptic vesicle endocytosis by localizing synaptojanin*. *Neuron*, 2003. **40**(4): p. 749-62.
138. Dickman, D.K., J.A. Horne, I.A. Meinertzhagen, and T.L. Schwarz, *A slowed classical pathway rather than kiss-and-run mediates endocytosis at synapses lacking synaptojanin and endophilin*. *Cell*, 2005. **123**(3): p. 521-33.
139. Wabnig, S., J.F. Liewald, S.C. Yu, and A. Gottschalk, *High-Throughput All-Optical Analysis of Synaptic Transmission and Synaptic Vesicle Recycling in Caenorhabditis elegans*. *PLoS One*, 2015. **10**(8): p. e0135584.
140. Gotzke, H., et al., *The ALFA-tag is a highly versatile tool for nanobody-based bioscience applications*. *Nat Commun*, 2019. **10**(1): p. 4403.
141. Le, T.L., A.S. Yap, and J.L. Stow, *Recycling of E-cadherin: a potential mechanism for regulating cadherin dynamics*. *J Cell Biol*, 1999. **146**(1): p. 219-32.
142. Shapiro, L., J. Love, and D.R. Colman, *Adhesion molecules in the nervous system: structural insights into function and diversity*. *Annu Rev Neurosci*, 2007. **30**: p. 451-74.
143. Kamiguchi, H., et al., *The neural cell adhesion molecule L1 interacts with the AP-2 adaptor and is endocytosed via the clathrin-mediated pathway*. *J Neurosci*, 1998. **18**(14): p. 5311-21.
144. Minana, R., et al., *Neural cell adhesion molecule is endocytosed via a clathrin-dependent pathway*. *Eur J Neurosci*, 2001. **13**(4): p. 749-56.

145. Sotnikov, O.S., V.V. Malashko, and G.I. Rybakova, *Syncytial coupling of neurons in tissue culture and early ontogenesis*. *Neurosci Behav Physiol*, 2008. **38**(4): p. 323-31.
146. Sotnikov, O.S., N.M. Paramonova, and L.I. Archakova, *Ultrastructural analysis of interneuronal syncytial perforations*. *Cell Biol Int*, 2010. **34**(4): p. 361-4.
147. Sotnikov, O.S., G.I. Rybakova, and I.A. Solov'eva, *The question of the fusion of neuron processes*. *Neurosci Behav Physiol*, 2008. **38**(8): p. 839-43.
148. Gonzalez Santander, R., G. Martinez Cuadrado, and M. Rubio Saez, *Exceptions to Cajal's neuron theory: communicating synapses*. *Acta Anat (Basel)*, 1988. **132**(1): p. 74-6.
149. Gonzalez Santander, R., G. Martinez Cuadrado, M.V. Toledo Lobo, and F.J. Martinez Alonso, *Communicating synapses: types and functional interpretation. Exceptions to Cajal's neuron theory*. *Acta Anat (Basel)*, 1991. **142**(3): p. 249-60.
150. Idone, V., et al., *Repair of injured plasma membrane by rapid Ca²⁺-dependent endocytosis*. *J Cell Biol*, 2008. **180**(5): p. 905-14.
151. Tuck, E. and V. Cavalli, *Roles of membrane trafficking in nerve repair and regeneration*. *Commun Integr Biol*, 2010. **3**(3): p. 209-14.
152. Eddleman, C.S., et al., *Endocytotic formation of vesicles and other membranous structures induced by Ca²⁺ and axolemmal injury*. *J Neurosci*, 1998. **18**(11): p. 4029-41.
153. Gibson, D.G., et al., *Enzymatic assembly of DNA molecules up to several hundred kilobases*. *Nat Methods*, 2009. **6**(5): p. 343-5.
154. Frokjaer-Jensen, C., M.W. Davis, M. Ailion, and E.M. Jorgensen, *Improved Mos1-mediated transgenesis in C. elegans*. *Nat Methods*, 2012. **9**(2): p. 117-8.
155. Frokjaer-Jensen, C., et al., *Single-copy insertion of transgenes in Caenorhabditis elegans*. *Nat Genet*, 2008. **40**(11): p. 1375-83.
156. Chronis, N., M. Zimmer, and C.I. Bargmann, *Microfluidics for in vivo imaging of neuronal and behavioral activity in Caenorhabditis elegans*. *Nat Methods*, 2007. **4**(9): p. 727-31.
157. Burbea, M., et al., *Ubiquitin and AP180 regulate the abundance of GLR-1 glutamate receptors at postsynaptic elements in C. elegans*. *Neuron*, 2002. **35**(1): p. 107-20.
158. Togashi, H., T. Sakisaka, and Y. Takai, *Cell adhesion molecules in the central nervous system*. *Cell Adh Migr*, 2009. **3**(1): p. 29-35.
159. Margolis, R.L. and C.A. Ross, *Expansion explosion: new clues to the pathogenesis of repeat expansion neurodegenerative diseases*. *Trends Mol Med*, 2001. **7**(11): p. 479-82.
160. Zoghbi, H.Y. and H.T. Orr, *Glutamine repeats and neurodegeneration*. *Annu Rev Neurosci*, 2000. **23**: p. 217-47.

161. Pecho-Vrieseling, E., et al., *Transneuronal propagation of mutant huntingtin contributes to non-cell autonomous pathology in neurons*. Nat Neurosci, 2014. **17**(8): p. 1064-72.
162. Babcock, D.T. and B. Ganetzky, *Transcellular spreading of huntingtin aggregates in the Drosophila brain*. Proc Natl Acad Sci U S A, 2015. **112**(39): p. E5427-33.
163. Chanaday, C., et al., *The Synaptic Vesicle Cycle Revisited: New Insights into the Modes and Mechanisms*. The Journal of Neuroscience, 2019. **39**(42): p. 8209-16.